

The CD3 Conformational Change in the $\gamma\delta$ T Cell Receptor Is Not Triggered by Antigens but Can Be Enforced to Enhance Tumor Killing

Elaine P. Dopfer,^{1,2} Frederike A. Hartl,^{1,2} Hans-Heinrich Oberg,³ Gabrielle M. Siegers,^{1,2,4} O. Sascha Yousefi,^{1,2,5} Sylvia Kock,⁶ Gina J. Fiala,^{1,2,5} Beatriz Garcillán,⁷ Andrew Sandstrom,⁸ Balbino Alarcón,⁹ Jose R. Regueiro,⁷ Dieter Kabelitz,³ Erin J. Adams,⁸ Susana Minguet,^{1,2} Daniela Wesch,³ Paul Fisch,⁶ and Wolfgang W.A. Schamel^{1,2,*}

¹Department of Molecular Immunology, Faculty of Biology, BIOS Centre for Biological Signaling Studies and Centre of Chronic Immunodeficiency (CCI), University of Freiburg, Schänzlestrasse 18, 79108 Freiburg, Germany

²Max Planck Institute of Immunobiology and Epigenetics, Stübweg 51, 79104 Freiburg, Germany

³Institute of Immunology, Christian-Albrechts University of Kiel, 24105 Kiel, Germany

⁴Robarts Research Institute, Department of Anatomy and Cell Biology, Robarts Research Institute, Western University, London, ON N6A 5B7, Canada

⁵Spemann Graduate School of Biology and Medicine (SGBM), Albert Ludwigs University Freiburg, 79104 Freiburg, Germany

⁶Institute of Pathology, University Medical Center Freiburg, 79106 Freiburg, Germany

⁷Faculty of Medicine, Universidad Complutense, 28040 Madrid, Spain

⁸Department of Biochemistry and Molecular Biology, University of Chicago, IL 60637, USA

⁹Centro de Biología Molecular Severo Ochoa, Consejo Superior de Investigaciones Científicas, Universidad Autónoma de Madrid, 28049 Madrid, Spain

*Correspondence: wolfgang.schamel@biologie.uni-freiburg.de

<http://dx.doi.org/10.1016/j.celrep.2014.04.049>

This is an open access article under the CC BY-NC-ND license (<http://creativecommons.org/licenses/by-nc-nd/3.0/>).

SUMMARY

Activation of the T cell receptor (TCR) by antigen is the key step in adaptive immunity. In the $\alpha\beta$ TCR, antigen induces a conformational change at the CD3 subunits (CD3 CC) that is absolutely required for $\alpha\beta$ TCR activation. Here, we demonstrate that the CD3 CC is not induced by antigen stimulation of the mouse G8 or the human V γ 9V δ 2 $\gamma\delta$ TCR. We find that there is a fundamental difference between the activation mechanisms of the $\alpha\beta$ TCR and $\gamma\delta$ TCR that map to the constant regions of the TCR $\alpha\beta$ / $\gamma\delta$ heterodimers. Enforced induction of CD3 CC with a less commonly used monoclonal anti-CD3 promoted proximal $\gamma\delta$ TCR signaling but inhibited cytokine secretion. Utilizing this knowledge, we could dramatically improve in vitro tumor cell lysis by activated human $\gamma\delta$ T cells. Thus, manipulation of the CD3 CC might be exploited to improve clinical $\gamma\delta$ T cell-based immunotherapies.

INTRODUCTION

$\alpha\beta$ T cells use their $\alpha\beta$ T cell antigen receptor ($\alpha\beta$ TCR) to recognize an almost infinite number of peptide antigens presented by major histocompatibility complex molecules (pMHC) on antigen-presenting cells (APCs). In contrast, $\gamma\delta$ T cells have a rather limited germline-encoded receptor repertoire. Their $\gamma\delta$ TCRs in part recognize stress-induced self-antigens, lipids, or pyrophosphates that are secreted by some microbes or are overproduced in tumor cells (Bonneville et al., 2010; Chien and Konigshofer,

2007; Vantourout and Hayday, 2013). $\gamma\delta$ TCRs can also deliver ligand-independent signals for $\gamma\delta$ T cell development in the thymus (Jensen et al., 2008).

In mice, 1% of the $\gamma\delta$ T cells recognize the nonclassical MHC class I molecule T22, which is expressed on activated cells, such as lipopolysaccharide (LPS)-stimulated B cells (Crowley et al., 2000; Matis et al., 1987). One example is the G8 $\gamma\delta$ TCR that uses its CDR3 δ loop to bind with high affinity to T22 (Adams et al., 2005; Crowley et al., 2000; Weintraub et al., 1994).

In human blood, the main subset of $\gamma\delta$ T cells is V γ 9V δ 2 that accounts for 2%–10% of all T cells. The V γ 9V δ 2 TCR recognizes self and foreign nonpeptidic phosphorylated small organic compounds, collectively termed phosphoantigens (Bukowski et al., 1995, 1998; Constant et al., 1994; Espinosa et al., 2001; Tanaka et al., 1995). V γ 9V δ 2 T cells are also stimulated by tumor cells, such as the Daudi B cell lymphoma (Fisch et al., 1997), that likely express high levels of phosphoantigens (Gober et al., 2003). Antigen recognition and tumor cell killing by V γ 9V δ 2 T cells can be enhanced with aminobisphosphonates, such as zoledronate (Roelofs et al., 2009), which increase accumulation of endogenous phosphoantigen.

TCRs consist of a clonotypic TCR $\alpha\beta$ or TCR $\gamma\delta$ heterodimer, two CD3 dimers (CD3 $\delta\epsilon$, CD3 $\gamma\epsilon$), and a $\zeta\zeta$ dimer. TCR $\alpha\beta$ and TCR $\gamma\delta$ chains contain variable (V) immunoglobulin domains that bind to the antigen, and constant (C) domains that associate with CD3. CD3 and ζ contain tyrosines in their cytoplasmic tails that are phosphorylated upon antigen binding to TCR $\alpha\beta$ or TCR $\gamma\delta$. In this report, “TCR $\alpha\beta$ ” or “TCR $\gamma\delta$ ” denote the TCR $\alpha\beta$ or TCR $\gamma\delta$ heterodimers, and “ $\alpha\beta$ TCR” or “ $\gamma\delta$ TCR” the complete TCRs including the CD3 and ζ chains. Although similar in domain structure, the architecture of $\gamma\delta$ TCRs differs from that of $\alpha\beta$ TCRs (see the Discussion).

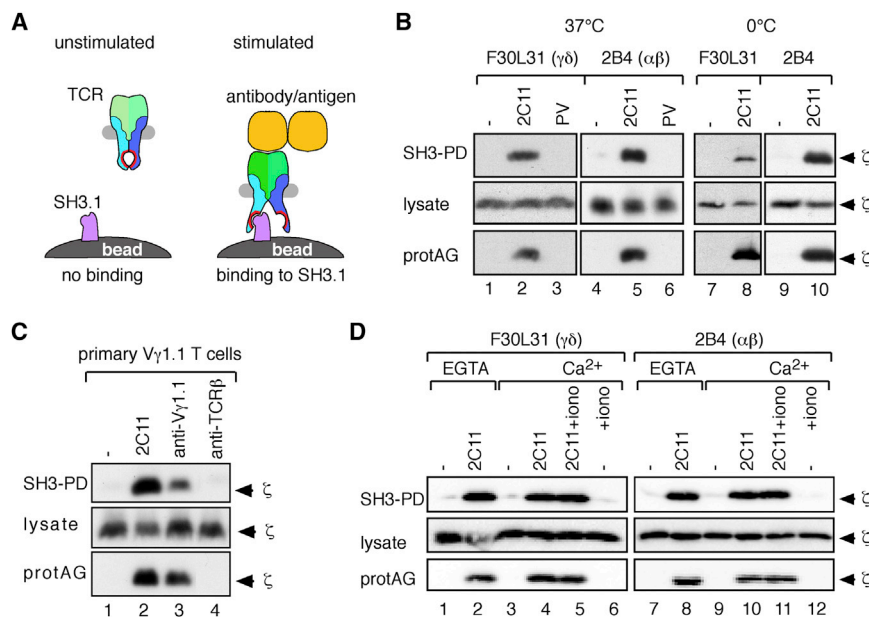


Figure 1. CD3 Conformational Change Induction at Murine $\gamma\delta$ TCRs

(A) Schematic of the SH3-PD assay.

(B) The murine $\gamma\delta$ T cell hybridoma F30L31 and $\alpha\beta$ T cell hybridoma 2B4 were left untreated (–) and stimulated for 5 min at 37°C or 0°C with 5 μ g/ml anti-CD3 mAb 2C11 or for 5 min with pervanadate (PV). After lysis, one aliquot of lysates was incubated with SH3 beads and another with protein A- and protein G beads. Lysates and bead-purified proteins were analyzed by anti- ζ WB (n > 3).

(C) Pooled thymocytes and splenocytes of TCR $\beta^{-/-}$ V γ 1.1tg mice were stimulated at 37°C with anti-CD3 (2C11), anti-V γ 1.1, or anti-TCR β (H57-597) antibodies. The samples were treated as in (B) (n = 3).

(D) F30L31 and 2B4 cells were left untreated (–) or stimulated with 2C11 in the presence of 4 mM EGTA. Additionally, cells were left untreated and stimulated with 2C11, with 2C11 plus 1 μ g/ml ionomycin or with ionomycin alone in the presence of 0.9 mM Ca²⁺. After lysis, one aliquot of lysates was incubated with SH3 beads and another with protein A and protein G beads. In the lysis and washing buffers, EGTA or Ca²⁺ were present as indicated. Lysates and bead-purified proteins were analyzed by anti- ζ WB (n = 3).

Stimulation of the $\alpha\beta$ TCR and the $\gamma\delta$ TCR initiates intracellular signaling cascades, such as Ca²⁺ influx, PI3K/AKT, Ras/Erk, and NF κ B pathways that are extensively studied. However, how antigen binding to TCR $\alpha\beta$ or TCR $\gamma\delta$ is communicated to the cytosolic tails of CD3 and ζ is less well understood (Kuhns and Davis, 2012). It has been suggested that the $\alpha\beta$ TCR exists in two conformations. In the closed conformation, adopted by the unstimulated $\alpha\beta$ TCR, the cytosolic tails of CD3 and ζ might be shielded from phosphorylation (Minguet and Schamel, 2008). In the open conformation, induced by productive antigen or antibody binding, CD3 and ζ phosphorylation might be promoted by an unknown mechanism.

The experimental assay to measure this CD3 conformational change (CD3 CC) makes use of the increased accessibility of a proline-rich sequence (PRS) in the CD3 ϵ cytoplasmic tail. In the closed conformation, the PRS cannot bind to the first SH3 domain of the adaptor protein Nck. In contrast, in the open conformation the PRS is accessible and thus binds to this SH3 domain (Borroto et al., 2013, 2014; de la Cruz et al., 2011; Gil et al., 2002, 2005; Martínez-Martín et al., 2009; Minguet et al., 2007). In fact, PRS exposure is correlated with an overall rearrangement in the structure of the CD3 and ζ cytoplasmic tails (Risueño et al., 2008).

The CD3 CC, as measured by PRS exposure, precedes CD3 phosphorylation (Gil et al., 2002) and is required for $\alpha\beta$ T cell activation (Minguet et al., 2007), in that engineered ligands that could not induce the CD3 CC did not result in $\alpha\beta$ TCR phosphorylation and downstream signaling. Likewise, point mutations in the extracellular part of CD3 ϵ that do not allow the outside-in transmission of the CD3 CC, such as CD3 ϵ K76T or CD3 ϵ C80G, inhibit $\alpha\beta$ TCR signaling in vitro and in vivo (Martínez-Martín et al., 2009). Thus, without the CD3 CC, an $\alpha\beta$ TCR cannot be activated.

CD3 ϵ also contains a cytosolic basic-rich sequence that has been proposed to interact with the acidic lipids of the inner mem-

brane leaflet, shielding the cytoplasmic CD3 ϵ tyrosines from phosphorylation in the unstimulated $\alpha\beta$ TCR (Deford-Watts et al., 2009; Xu et al., 2008). Signaling by the $\alpha\beta$ TCR leads to Ca²⁺-influx neutralizing the negative lipid head groups and thus, freeing the CD3 ϵ cytosolic domain from the membrane and promoting sustained signaling after the initial $\alpha\beta$ TCR trigger (Shi et al., 2013). Whether Ca²⁺ ions can influence the exposure of the PRS is currently unknown.

To date, studies exploring the induction of the CD3 CC in $\gamma\delta$ TCRs are lacking. Here, we tested if the CD3 CC can be induced in the mouse and human $\gamma\delta$ TCR and whether it regulates $\gamma\delta$ T cell activation.

RESULTS

Murine $\gamma\delta$ TCRs Undergo a Conformational Change at CD3 ϵ upon Antibody Stimulation

To assess whether the $\gamma\delta$ TCR undergoes the CD3 CC upon stimulation, we used the murine $\gamma\delta$ T cell line F30L31 expressing a V γ 1.1 TCR, and as a control the mouse $\alpha\beta$ T cell line 2B4. We carried out an SH3 pull-down (PD) assay using the first SH3 domain of Nck (Figure 1A). Anti- ζ western blotting showed that resting, unstimulated TCRs did not bind to the SH3-coupled beads (Figure 1B, lanes 1 and 4), whereas stimulation with the anti-CD3 monoclonal antibody (mAb) 145-2C11 (2C11) at 37°C induced binding of the $\gamma\delta$ TCR and the $\alpha\beta$ TCR to SH3 beads (lanes 2 and 5). Stimulation with the phosphatase inhibitor pervanadate (PV) did not trigger binding of the TCRs to SH3 (lanes 3 and 6). As a further control, we incubated the lysates with protein A- and G-coupled beads to immunoprecipitate the TCRs via the bound anti-CD3 mAb (lower panels). In addition, anti-TCR $\gamma\delta$ antibody stimulation also induced $\gamma\delta$ TCR binding to SH3 (Figure S1A). A hallmark of the CD3 CC is its independence from any metabolic process (Gil et al., 2002; Minguet et al.,

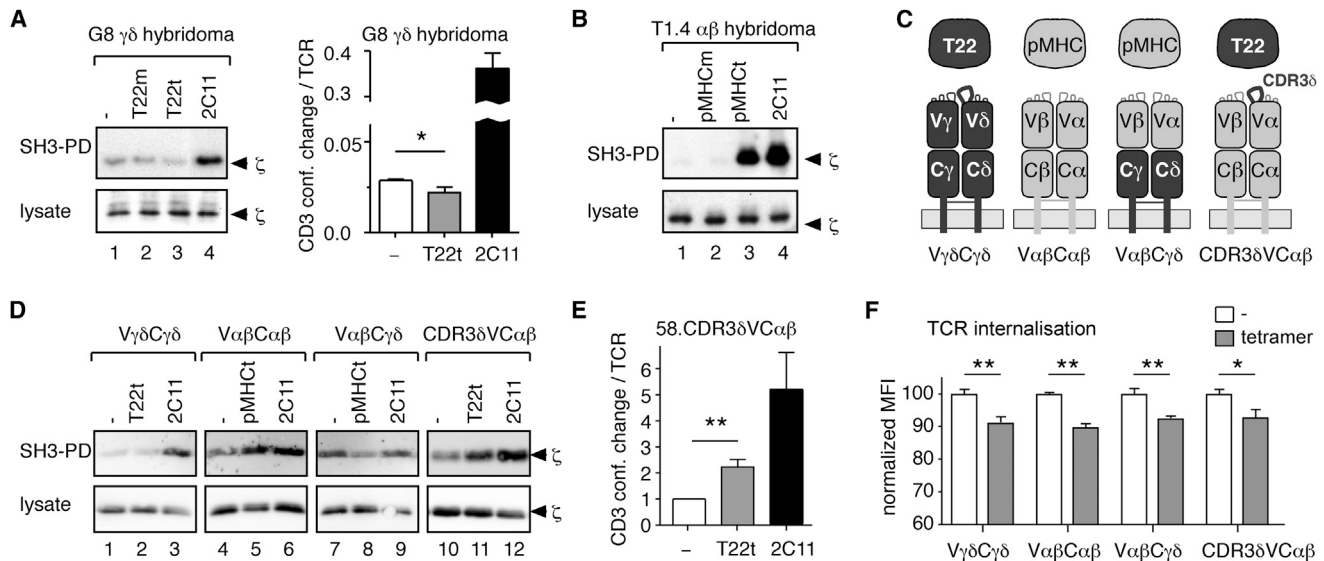


Figure 2. The Murine G8 $\gamma\delta$ TCR Does Not Undergo the CD3 CC upon Antigenic Stimulation

(A) G8 $\gamma\delta$ hybridoma cells were stimulated at 37°C with 5 μ g/ml T22 monomer (T22m), tetramer (T22t) or anti-CD3 (2C11), and the SH3-PD was performed. The ratio of SH3-bound TCR to total TCR (anti-CD3 IP) was calculated using the Odyssey infrared imager. The mean \pm SD is shown (n = 3). Significances were determined by the Student's t test to compare unstimulated versus T22t stimulated samples; *p < 0.05.

(B) T1.4 $\alpha\beta$ hybridoma cells were incubated with 500 nM H2-K^d-pepABA monomer or 5 nM H2-K^d-pepABA tetramer, or 5 μ g/ml 2C11, and the SH3-PD was performed (n = 3).

(C) Schematic picture of the murine WT and chimeric TCRs. The domains of the G8 $\gamma\delta$ TCR are depicted in dark gray, including the T22-binding CDR3 δ loop derived from the G8 $\gamma\delta$ TCR; the domains of the $\alpha\beta$ TCR are in light gray.

(D) The 58 $\alpha^- \beta^-$ transductants as indicated were stimulated with 5 μ g/ml T22 tetramers, H2-K^d-pepABA (pMHC) tetramers or anti-CD3 (2C11), and the SH3-PD was performed (n = 2).

(E) Using the 58.CDR3 δ VC $\alpha\beta$ cells, the statistics from six experiments as in (D) was performed as in (A) normalizing to the unstimulated samples; **p < 0.01.

(F) The 58 $\alpha^- \beta^-$ transductants were stimulated in triplicates for 2 hr as in (D). Subsequently, cells were stained with anti-CD3 ϵ (2C11) mAb for flow cytometry (four measurements are pooled). The mean \pm SEM is shown. Significances between unstimulated and tetramer-stimulated cells were determined by the Student's t test; *p < 0.05; **p < 0.01.

2007); thus, it even took place at 0°C (Figure 1B, lanes 8 and 10). This indicates that the induced binding of the $\gamma\delta$ TCR to SH3 reflects structural changes in CD3 ϵ (the CD3 CC), as previously described for the $\alpha\beta$ TCR.

In primary ex vivo $\gamma\delta$ T cells from TCR $\beta^{-/-}$ -V γ 1.1tg mice, both anti-CD3 and anti-V γ 1.1, but not anti-TCR β mAbs, induced binding of the $\gamma\delta$ TCR to the SH3 beads (Figure 1C). Thus, mouse $\gamma\delta$ TCRs undergo conformational changes at CD3 upon stimulation with $\gamma\delta$ TCR- and CD3-specific antibodies.

Next, we tested whether the TCR-mediated Ca²⁺ influx, which was proposed to expose the cytosolic tail of CD3 in case of the $\alpha\beta$ TCR (Shi et al., 2013), was involved in the induction of the CD3 CC, as measured by the SH3-PD assay (Figure 1D). To this end, we left F30L31 $\gamma\delta$ and 2B4 $\alpha\beta$ T cells unstimulated (–) or stimulated them with anti-CD3 (2C11) in the absence of Ca²⁺ ions in the medium, lysis, and washing buffers (all containing EGTA). Alternatively, the stimulation was performed in the presence of Ca²⁺ in these buffers and an optional treatment of the cells with ionomycin to allow Ca²⁺ to flux into the cytosol. The presence or absence of Ca²⁺ did not influence the amount of TCRs bound to the SH3-coupled beads, neither basally nor upon antibody stimulation (Figure 1D). Thus, Ca²⁺-induced structural changes in the TCR are not related to the CD3 CC, and the CD3 CC most likely is upstream of TCR-induced Ca²⁺ influx.

Antigen Binding to Mouse G8 $\gamma\delta$ TCRs Does Not Trigger the CD3 CC

Next, we tested whether natural antigens induce the structural rearrangement of CD3 ϵ in the $\gamma\delta$ TCR. For this purpose, we made use of a murine hybridoma cell line expressing the G8 $\gamma\delta$ TCR (Bluestone et al., 1988) specific for the MHC I-like molecule T22 (Schild et al., 1994). Upon stimulation of the G8 $\gamma\delta$ hybridoma with biotinylated T22 monomers or tetramers for 5 min at 37°C, the CD3 CC was not induced (Figure 2A, lanes 2 and 3). Surprisingly, tetramer binding to the G8 $\gamma\delta$ TCR significantly reduced the CD3 CC, as compared to the basal level (Figures 2A, right panel, and S1B). As a control, we used anti-CD3 stimulation to trigger the CD3 CC. In contrast to the $\gamma\delta$ TCR, MHC class I H2-K^d-pepABA (pMHC) tetramers induced the CD3 CC in the mouse T1.4 $\alpha\beta$ hybridoma (Figure 2B), as previously described (Minguet et al., 2007). The G8 $\gamma\delta$ hybridoma cells bound similar amounts of antigen tetramers as the T1.4 $\alpha\beta$ hybridoma cells (Figure S1C); thus, low levels of T22 tetramer binding were not responsible for the lack of CD3 CC detection in the $\gamma\delta$ TCR.

Next we used LPS-activated splenic B cells expressing endogenous T22 as antigen-presenting cells (APCs) (Spaner et al., 1995). Again, stimulation of the G8 $\gamma\delta$ hybridoma tended to reduce the CD3 CC (Figure S1D). Thus, using the

best-characterized antigen for a specific $\gamma\delta$ TCR, our results showed that a natural antigen did not induce the CD3 CC and even evoked a slight reduction in the amount of conformationally changed TCRs upon stimulation.

The Capacity to Undergo the CD3 CC Maps to the TCR $\alpha\beta$ Constant Regions

To test whether the $\gamma\delta$ cellular environment inhibited CD3 CC induction, we expressed the G8 $\gamma\delta$ TCR in the murine $\alpha\beta$ hybridoma 58 $\alpha^- \beta^-$ defective for TCR α and TCR β expression, yielding 58.V $\gamma\delta$ C $\gamma\delta$ cells (Figure 2C, left panel, and S2). Stimulation with T22 tetramers did not induce the CD3 CC (Figure 2D, lanes 1–3), indicating that the T22–G8 $\gamma\delta$ TCR system intrinsically lacks the ability to undergo the CD3 CC.

Hence, our findings raised the question whether, in contrast to conventional pMHC tetramers, the T22 antigen is in principle incapable of inducing the CD3 CC, or whether it is intrinsic to the G8 $\gamma\delta$ TCR that productive antigen engagement does not result in the CD3 CC. To test these opposing possibilities, we generated chimeric $\gamma\delta$ - $\alpha\beta$ TCRs and expressed them in 58 $\alpha^- \beta^-$ cells (Figures 2C and S2). 58.V $\alpha\beta$ C $\alpha\beta$ cells express the T1 $\alpha\beta$ TCR, 58.V $\alpha\beta$ C $\gamma\delta$ cells a chimeric TCR with the V regions from T1 TCR $\alpha\beta$ and the C regions from G8 TCR $\gamma\delta$, and 58.CDR3 δ VC $\alpha\beta$ cells express the 172 $\alpha\beta$ TCR with the T22-binding CDR3 δ region of the G8 TCR δ chains as reported (Adams et al., 2008).

Strikingly, pMHC-tetramer stimulation of the chimeric V $\alpha\beta$ C $\gamma\delta$ TCR did not induce the CD3 CC, but rather reduced the basal level (Figure 2D, lanes 7–9). In contrast, in the CDR3 δ VC $\alpha\beta$ the T22 tetramers induced the CD3 CC (Figure 2D, lanes 10–12) that was statistically significant compared to unstimulated cells (Figure 2E). Thus, neither the different binding geometry nor the different affinity of the T22- $\gamma\delta$ TCR compared to the pMHC- $\alpha\beta$ TCR interaction determined CD3 CC induction. Rather the G8 $\gamma\delta$ TCR is intrinsically different from the $\alpha\beta$ TCR, because the constant regions of the TCR $\gamma\delta$ chains do not transmit the conformational change to CD3 upon antigen binding.

Ligand-induced TCR activation leads to intracellular signaling, causing TCR internalization. Our wild-type (WT) and chimeric TCRs were internalized upon stimulation with their corresponding T22 or pMHC tetramers, indicating that induction of the CD3 CC was not required for $\gamma\delta$ TCR activation (Figure 2F).

Triggering of the CD3 Conformational Change in the Human V γ 9V δ 2 TCR

Next, we tested whether the CD3 CC can be induced in a human V γ 9V δ 2 $\gamma\delta$ T cell clone (Fisch et al., 1990b; Fisch et al., 1997). Stimulation with the anti-CD3 mAb UCHT1 triggered the CD3 CC (Figure 3A, lanes 2 and 8). However, the more commonly used anti-CD3 mAb OKT3 showed markedly reduced potency in the induction of the CD3 CC at 37°C and was completely inactive at 0°C (lanes 3 and 9). However, similar amounts of TCR were bound by UCHT1 and OKT3, because protein A- and G-coupled beads precipitated similar amounts of antibody-bound TCRs (ζ chain detection, lower panels). As expected, anti-TCR $\gamma\delta$ but not pervanadate (PV) stimulation induced the CD3 CC (lanes 6 and 4). The same result was ob-

tained with a different V γ 9V δ 2 T cell clone (data not shown). Similarly, when using human freshly isolated, purified $\gamma\delta$ T cells, OKT3 was a less potent inducer of the CD3 CC as compared to UCHT1 or anti-TCR $\gamma\delta$ (Figure 3B).

In contrast, UCHT1 and OKT3 equally induced the CD3 CC in human Jurkat $\alpha\beta$ T cells (Figure 3C, lanes 2 and 3). The lack of structural changes at CD3 in the $\gamma\delta$ TCR upon OKT3 stimulation could be due to the $\gamma\delta$ TCR itself or differing cellular environments in $\gamma\delta$ compared to $\alpha\beta$ T cells. To distinguish between these possibilities, we used a TCR β -deficient Jurkat cell line expressing the human V γ 9V δ 2 TCR (Jk.V γ 9V δ 2) (Alibaud et al., 2001). Again, UCHT1 was much more potent than OKT3 in triggering the CD3 CC (Figures 3C, lanes 5 and 6, S3A, and S3B). In conclusion, UCHT1 was a much more potent trigger for the CD3 CC in the human V γ 9V δ 2 TCR than OKT3, and differential induction of the CD3 CC in the human $\gamma\delta$ TCR compared to the human $\alpha\beta$ TCR is due to intrinsic properties of these TCRs.

The human V γ 9V δ 2 TCR is naturally stimulated by phosphoantigens (Bukowski et al., 1995; Constant et al., 1994). We stimulated the V γ 9V δ 2 T cell clone with the two most commonly used synthetic phosphoantigens bromohydrin pyrophosphate (BrHPP) or isopentenyl pyrophosphate (IPP) (Espinosa et al., 2001) and could not detect the CD3 CC above background (Figure 3D, lanes 2 and 3). As a positive control, UCHT1 triggered the CD3 CC (lane 4). Furthermore, stimulation with Daudi cells (Fisch et al., 1997) or zoledronate (ZOL)-pulsed Daudi cells with increased levels of endogenous phosphoantigens (Roelofs et al., 2009) did not induce the CD3 CC (Figures 3E, lanes 2 and 3, and S3C).

Next, we quantified tumor necrosis factor (TNF)- α production using the same concentration of the stimuli as for the CD3 CC assay (Figure 3F). UCHT1 induced TNF- α production to an extent similar that obtained via stimulation by Daudi or Daudi+ZOL, and 4-fold less compared to IPP. Hence, induction of the CD3 CC did not correlate with TNF- α production, indicating that CD3 CC induction is not required for TNF- α production by $\gamma\delta$ T cells. As a control, stimulation with Daudi cells neither induced the CD3 CC in the V γ 9V δ 2 clone nor activated an $\alpha\beta$ T cell clone (Figures 3E and 3F).

In conclusion, using phosphoantigens as well as antigen-expressing Daudi cells, we did not detect the CD3 CC in human V γ 9V δ 2 TCRs. This is in strong contrast to the $\alpha\beta$ TCR where stimulation with pMHC tetramers and APCs induce this conformational change (de la Cruz et al., 2011; Gil et al., 2005, 2008; Minguet et al., 2007; Risueño et al., 2005, 2006).

CD3 CC Induction at the $\gamma\delta$ TCR Correlates with Activation of TCR-Proximal Signaling Events

To investigate the influence of the CD3 CC on $\gamma\delta$ TCR activation, we compared the effects of UCHT1 and OKT3 on human $\gamma\delta$ T cells using different functional readouts. To ensure that equal numbers of $\gamma\delta$ TCRs were stimulated, we used both mAbs at 5 μ g/ml—a concentration at which similar amounts of $\gamma\delta$ TCRs were bound to UCHT1 and OKT3 (Figure 3A). Although UCHT1 stimulation evoked a strong Ca²⁺ influx, OKT3 led to a much weaker response in the V γ 9V δ 2 T cell clone (Figure 4A) and in freshly isolated, purified human $\gamma\delta$ T cells (Figure 4B). In $\alpha\beta$

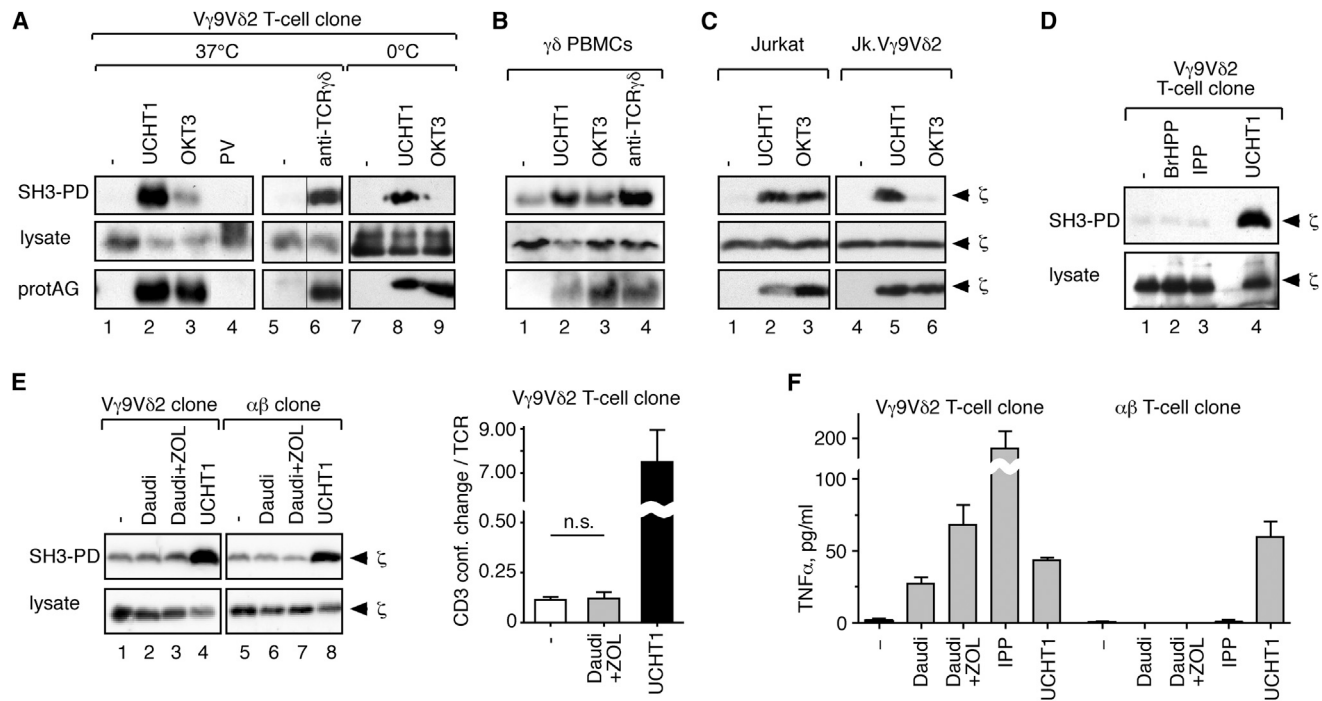


Figure 3. CD3 CC Induction at the Human V γ 9V δ 2 TCR

(A) A human V γ 9V δ 2 T cell clone was left untreated or stimulated for 5 min at 37°C with 5 μ g/ml of the anti-CD3 mAbs UCHT1 and OKT3, pervanadate (PV) or anti-TCR $\gamma\delta$ (clone 5A6E9). Cells were also stimulated for 30 min at 0°C. After lysis, the SH3-PD was performed ($n > 3$).

(B) Freshly isolated, purified human $\gamma\delta$ T cells ($\gamma\delta$ PBMCs) were stimulated for 5 min at 37°C with 5 μ g/ml UCHT1, OKT3, and anti-TCR $\gamma\delta$ mAbs, and the SH3-PD was performed ($n = 1$).

(C) Jurkat and Jk.V γ 9V δ 2 cells were stimulated for 30 min at 0°C with 5 μ g/ml UCHT1 and OKT3, and the SH3-PD was performed ($n > 3$).

(D) BrHPP (500 nM) or IPP (30 μ M) was added to the V γ 9V δ 2 clone. Cells were gently centrifuged and left at 37°C for 60 min or stimulated for 5 min with UCHT1 as above. Cells were mildly lysed using 0.3% Brij58. The SH3-PD was performed ($n > 3$).

(E) The human V γ 9V δ 2 and a human $\alpha\beta$ T cell clone were left unstimulated and stimulated for 30 min with Daudi cells, zoledronate (ZOL)-pulsed Daudi cells or as a control, with 5 μ g/ml UCHT1. The SH3-PD was performed ($n > 3$). The statistics were performed as in Figure 2A; n.s., not significant.

(F) The V γ 9V δ 2 (left) and $\alpha\beta$ (right) T cell clones were stimulated with Daudi, ZOL-pulsed Daudi cells, 30 μ M IPP, or 5 μ g/ml UCHT1 for 18 hr. TNF- α concentration was measured by ELISA ($n > 3$). The mean \pm SD is shown.

Jurkat cells in which both UCHT1 and OKT3 induced the CD3 CC (Figure 3C), both antibodies triggered a strong Ca²⁺ influx (Figure S4A).

Using a multiplexed bead assay, we assessed the phosphorylation kinetics of signaling proteins downstream of the TCR, such as Akt, Erk, and I κ B α . In the V γ 9V δ 2 T cell clone, UCHT1 triggered a transient and strong phosphorylation of all three proteins (Figure 4C). In sharp contrast, OKT3 stimulation led to a slow and gradual increase in phosphorylation. A similar result was obtained with human purified $\gamma\delta$ T cells (Figure S4B). In addition, V γ 9V δ 2 TCR downmodulation from the cell surface was slightly enhanced by UCHT1 compared to OKT3 (Figure S4C). We conclude that triggering of the CD3 CC in the $\gamma\delta$ TCR led to enhanced proximal signaling events, as compared to stimulation in the absence of the CD3 CC.

Deglycosylation of the V γ 9V δ 2 TCR Facilitates CD3 CC Induction and Ca²⁺ Influx

Because CD3 glycosylation differs between the $\gamma\delta$ TCR and $\alpha\beta$ TCR (Alarcon et al., 1987; Krangel et al., 1987; Siegers et al.,

2007), we tested whether deglycosylation of the $\gamma\delta$ TCR modifies the ability of OKT3 to trigger the CD3 CC. Treatment of the V γ 9V δ 2 T cell clone with N-acetyl neuraminidase (NA), to cleave sialic acid sugars, allowed CD3 CC induction by OKT3 (Figure 5A, lane 5). The $\gamma\delta$ -specific pattern of CD3 glycosylation is dependent on the expression of the TCR $\gamma\delta$ chains and not the cellular background (Siegers et al., 2007). In an $\alpha\beta$ cellular background (Jk.V γ 9V δ 2 cells) OKT3 was also unable to induce the CD3 CC in the $\gamma\delta$ TCR (Figure 3C). However, deglycosylation allowed the CD3 CC to take place (Figure S4D). Deglycosylation also increased the CD3 CC induced by UCHT1 (Figure 5A), indicating that this effect is not specific for OKT3.

Next, we tested whether supplementing OKT3 stimulation with the CD3 CC by deglycosylating the $\gamma\delta$ T cells influences TCR-induced signaling. Although OKT3 stimulation alone did not result in a measurable Ca²⁺ influx (Figure 5B), enhanced Ca²⁺ influx was detected when the V γ 9V δ 2 T cell clone was deglycosylated prior to OKT3 stimulation (Figure 5B). Thus, the specific glycosylation of the $\gamma\delta$ TCR controls inducibility of the CD3 CC and its associated signal transduction.

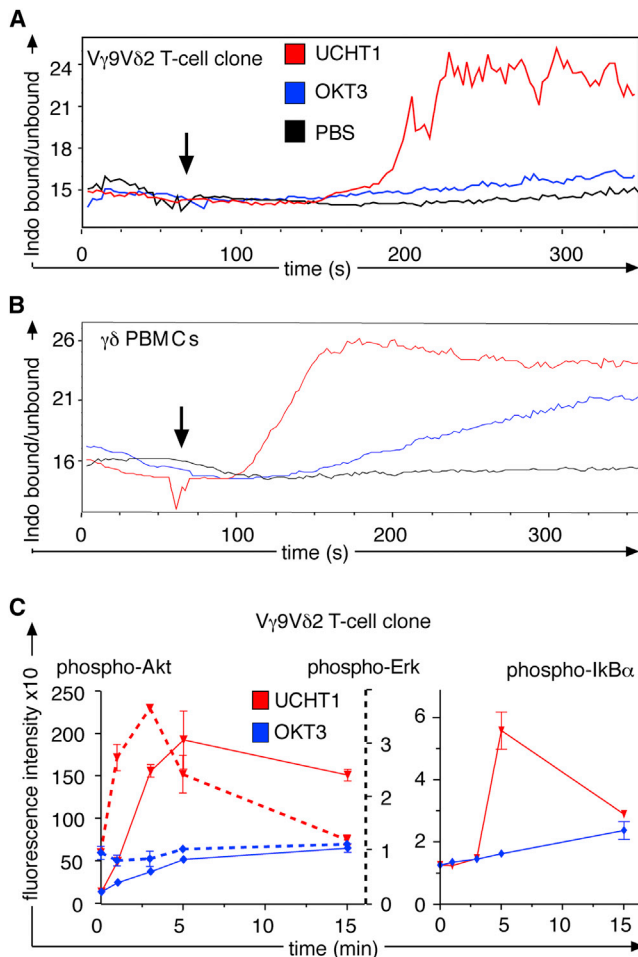


Figure 4. UCHT1, but Not OKT3, Stimulation Promotes TCR-Proximal Intracellular Signaling

(A) The human V γ 9V δ 2 T cell clone was loaded with Indo-1 and stimulated with 5 μ g/ml UCHT1 and OKT3. The Indo-1 ratio was integrated over 6 min and measured by flow cytometry.

(B) Human freshly isolated, purified $\gamma\delta$ T cells ($\gamma\delta$ PBMCs) were measured as in (A).

(C) The human V γ 9V δ 2 T cell clone was stimulated with 5 μ g/ml UCHT1 and OKT3 for 1, 3, 5, and 15 min. Phospho-Akt (solid line, y axis on left), phospho-Erk (dashed line, y axis on right), and phospho-I κ B α were measured by a multiplexed-bead assay performed on cell lysates. All panels were performed $n > 3$. The mean \pm SD is shown.

Multimerization of OKT3 Facilitates the CD3 CC, Thereby Enhancing Ca²⁺ Influx

For the $\alpha\beta$ TCR, antigen-TCR interactions of high valency favor the induction of the CD3 CC (Minguet and Schamel, 2008). In order to enable OKT3 to simultaneously bind to more than two $\gamma\delta$ TCRs, we costimulated with an anti- κ antibody that binds to the κ light chain of OKT3. Indeed, under these conditions the CD3 CC in the $\gamma\delta$ TCR was induced (Figure 5C, lane 6). Interestingly, anti- κ had little or no effect on UCHT1 induction of the CD3 CC (lanes 2 and 5). Accordingly, anti- κ treatment enabled OKT3-triggered Ca²⁺ influx in $\gamma\delta$ T cells (Figure 5D, upper panel). As a control, anti- κ did not significantly enhance Ca²⁺ influx stimulated by UCHT1 (lower panel). Likewise, OKT3 multimerization

using an anti-mouse immunoglobulin (Ig) G antibody led to CD3 CC induction and Ca²⁺ influx (Figures S4D and S4E). These experiments suggest that the differences in triggering signaling downstream of the $\gamma\delta$ TCR by soluble UCHT1 or OKT3 are due to their differential capacity to induce the CD3 CC.

$\gamma\delta$ TCRs Containing Mutant CD3 CC-Defective CD3 ϵ Chains Had Reduced Capability to Induce Ca²⁺ Influx

Next, we made use of two CD3 ϵ mutants, K76T and C80G, that weakly and a strongly inhibit induction of the CD3 CC (Figure 5E) (Martínez-Martín et al., 2009). WT and mutant murine CD3 ϵ chains were expressed in the mouse $\gamma\delta$ F30L31 cells, yielding F. ϵ WT, F. ϵ K76T, and F. ϵ C80G cells. By using IRES-GFP constructs, those cells expressing the exogenous CD3 ϵ can be identified. The GFP⁺ F. ϵ WT, F. ϵ K76T, and F. ϵ C80G cells expressed similar $\gamma\delta$ TCR levels on their surface (Figure S5A). When they were stimulated with anti-CD3 mAb, a strong correlation between the capacity to induce the CD3 CC and the extent of Ca²⁺ flux was observed (GFP⁺ gated cells, Figure 5F), again showing that Ca²⁺ influx is promoted by the CD3 CC.

Induction of the CD3 CC Suppresses CD69 Upregulation and Cytokine Secretion by $\gamma\delta$ T Cells

Next, we tested whether the CD3 CC is required for the activation of $\gamma\delta$ TCR-induced distal events such as upregulation of the activation markers CD69 and CD25, cytokine secretion or proliferation. To this end, we stimulated the murine F. ϵ WT, F. ϵ K76T, and F. ϵ C80G cells with anti-CD3; we found that CD69 and CD25 were induced in both WT and CD3 CC mutant CD3 ϵ -expressing $\gamma\delta$ T cells (Figure 6A; data not shown). In fact, significantly more cells upregulated CD69 when the CD3 CC was suppressed (Figure 6A).

To corroborate this finding in human cells, our V γ 9V δ 2 T cell clone was stimulated using soluble OKT3 and UCHT1 mAbs. Again, OKT3 led to a slightly better induction of CD69 and CD25 on the cell surface (Figure 6B). In human freshly isolated, purified $\gamma\delta$ T cells, CD69 and CD25 were upregulated to a similar extent by both soluble UCHT1 and OKT3 (Figure 6C).

At the same time, we measured cytokines secreted into the supernatant using a multiplexed bead assay. Surprisingly, OKT3 induced a much greater release of interferon (IFN)- γ and TNF- α as compared to UCHT1 at all concentrations tested (Figures 6D and S5B). In contrast, when we stimulated the $\alpha\beta$ T cell clone, which can undergo the CD3 CC induced by either UCHT1 or OKT3 stimulation, equal amounts of IFN- γ and TNF- α were secreted (Figure S5C). Next, we multimerized UCHT1 and OKT3 by adhesion to a plastic dish, promoting conditions in which OKT3 induces the CD3 CC. As expected, secretion of IFN- γ and TNF- α was similar in cells stimulated with plate-bound OKT3 or UCHT1 (Figure 6E).

Similar to cytokine secretion, soluble OKT3 induced stronger proliferation of short-term cultured human $\gamma\delta$ T cells than UCHT1 (Figures 6F and S5D).

Induction of the CD3 CC Promotes $\gamma\delta$ T Cell-Mediated Tumor Lysis

Because the CD3 CC differentially influences $\gamma\delta$ T cell activation, we asked whether V γ 9V δ 2 T cell effector functions, such

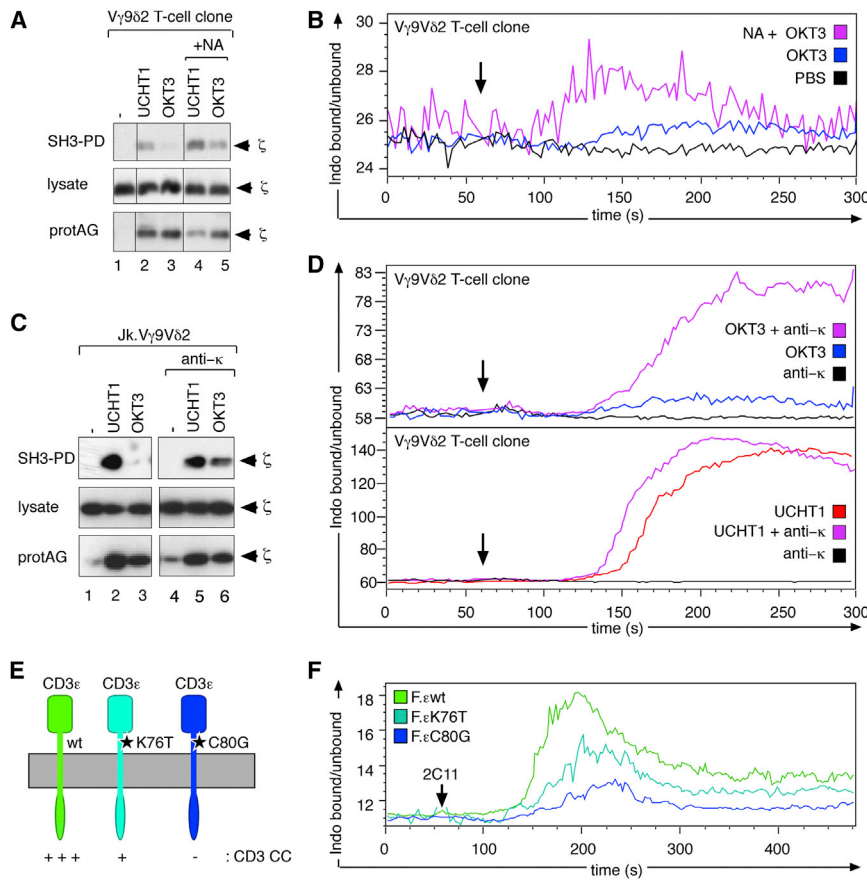


Figure 5. Induction of the CD3 CC Promotes Strong and Early Ca^{2+} Influx

(A) The human $V\gamma 9V\delta 2$ T cell clone was left untreated or deglycosylated with N-acetyl neuraminidase (NA) for 1 hr at $37^{\circ}C$. Subsequently, cells were stimulated with $5\ \mu g/ml$ UCHT1 or OKT3 for 5 min, and the SH3-PD was performed. (B) The $V\gamma 9V\delta 2$ T cell clone was left untreated or deglycosylated as in (A) and Ca^{2+} influx was measured upon OKT3 stimulation as before. (C) Jk. $V\gamma 9V\delta 2$ cells were stimulated with $5\ \mu g/ml$ UCHT1 or OKT3 with or without $2.5\ \mu g/ml$ anti- κ antibodies at $37^{\circ}C$, and the SH3-PD was performed. (D) For Ca^{2+} measurements using the $V\gamma 9V\delta 2$ T cell clone $2.5\ \mu g/ml$ anti- κ was added simultaneously with $5\ \mu g/ml$ UCHT1 or OKT3 as indicated. (E) Extent of CD3CC induction in the CD3 ϵ K76T and CD3 ϵ C80G mutants. (F) F. ϵ WT, F. ϵ K76T, and F. ϵ C80G cells were stimulated with $10\ \mu g/ml$ anti-mouse CD3 (2C11), and Ca^{2+} influx was measured while gating on the GFP $^{+}$ cells. All panels were performed $n = 3$, except (C) and (D), which were performed $n = 2$.

as tumor cell lysis, can be modulated by altering the CD3 CC. Stimulating $\gamma\delta$ T cell cultures from different healthy donors with 0.5 or $5\ \mu g/ml$ UCHT1 (which induces the CD3 CC) dramatically enhanced target cell lysis of the pancreatic tumor cell line Panc89 such that all tumor cells were lysed by 24 hr (Figures 7A, 7B, and S6). In contrast, OKT3 (which hardly triggers the CD3 CC) did not enhance tumor lysis. High concentrations of anti-CD3 mAbs induced cell death in activated $\gamma\delta$ T cells (Janssen et al., 1991; Kabelitz et al., 1994). Therefore, we examined lower mAb concentrations as well as different effector/target cell ratios. UCHT1, but not OKT3, augmented tumor cell killing by the $\gamma\delta$ T cells also at $0.05\ \mu g/ml$ (Figures 7B and S6A) and at different effector/target ratios using $\gamma\delta$ T cell cultures from different donors (Figure S6A). The effect of UCHT1 was dependent on $\gamma\delta$ T cells, because the growth of Panc89 cells alone was neither affected by UCHT1 nor by OKT3 (Figure 7C). In most cases OKT3 had a blocking effect on tumor cell lysis (Figures 7A, 7B, and S6A), as demonstrated previously (Fisch et al., 1990a). The differential activity of the two antibodies was neither due to differences in the induction of $\gamma\delta$ T cell apoptosis (Figure S6B) nor to antibody-dependent cellular cytotoxicity, because most $\gamma\delta$ T cells in our cultures (>97%) and Panc89 cells were negative for CD16 (data not shown). In conclusion, induction of the CD3 CC by UCHT1 drastically enhanced the tumor-killing capacity of human $\gamma\delta$ T cells.

Last, we transduced our $\gamma\delta$ T cell cultures with lentiviral vectors encoding murine CD3 ϵ WT and CD3 ϵ K76T. Murine CD3 ϵ C80G was not expressed well on human T cells (not shown). In both cultures, approximately 5% of the cells expressed the murine CD3 ϵ with a similar MFI (64 for CD3 ϵ WT and 67 for CD3 ϵ K76T, not shown). Stimulation with the anti-mouse CD3 mAb 2C11, which is a strong inducer of the CD3 CC (Figures 1 and 2), enhanced tumor cell killing by cells expressing CD3 ϵ WT more than those expressing CD3 ϵ K76T (Figure S6C). A similar result was obtained in a second experiment (Figure S6D). These experiments corroborate our finding that the CD3 CC promotes $\gamma\delta$ T cell cytotoxicity.

DISCUSSION

Here we show that a hallmark of the mechanism behind $\alpha\beta$ TCR triggering does not hold true for the three $\gamma\delta$ TCRs tested. The CD3 CC is required for $\alpha\beta$ TCR activation (Martínez-Martín et al., 2009; Minguet et al., 2007) and thus is induced by all agonistic pMHCs tested (de la Cruz et al., 2011; Gil et al., 2005, 2008; Minguet et al., 2007; Risueño et al., 2005, 2006, 2008). To investigate whether the $\alpha\beta$ TCR and $\gamma\delta$ TCR share the same activation principle, we used the best-described ligands available. First, using the murine G8 $\gamma\delta$ TCR we show that, despite T22 tetramer binding and triggering of signaling, the CD3 CC was not induced. In fact, T22 tetramer and APC stimulation even had the reverse effect in stabilizing the closed CD3 conformation, indicating that the $\gamma\delta$ TCR structure was sensitive to T22 binding. Second, the human $V\gamma 9V\delta 2$ TCR was activated by phosphoantigens, but the CD3 CC was not observed, although we used conditions that allow its detection in the

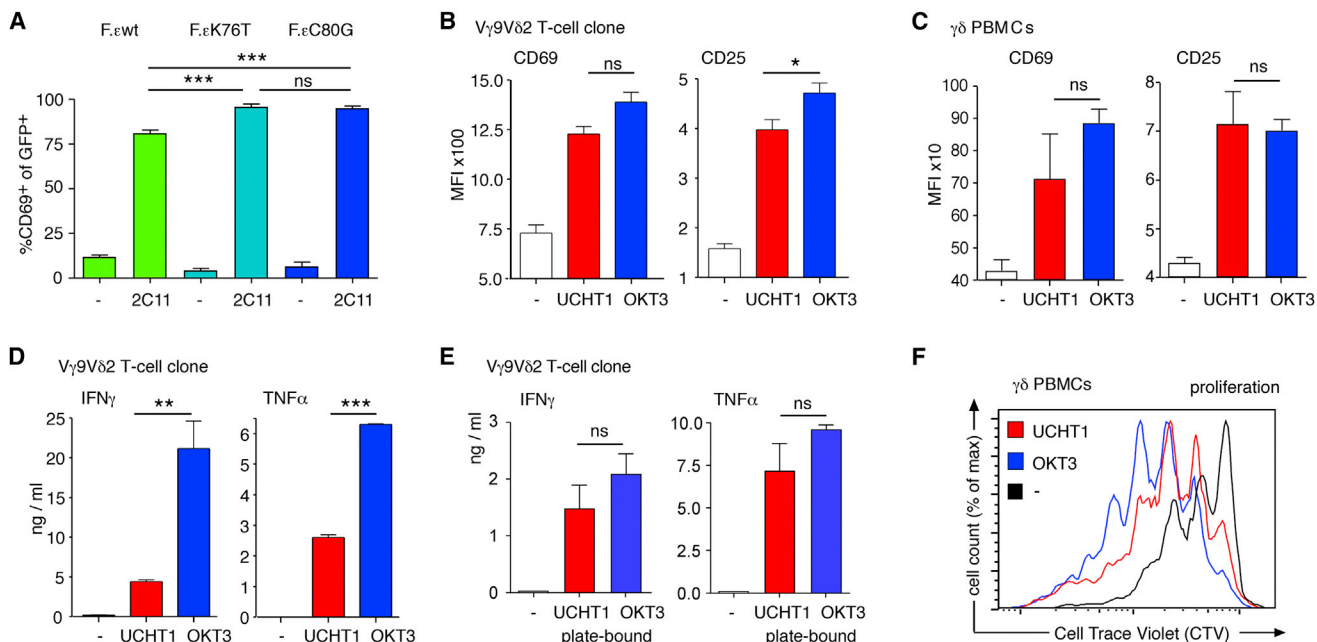


Figure 6. Induction of the CD3 CC Reduces Anti-CD3-Induced Cytokine Secretion in V γ 9V δ 2 T Cells

(A) F.CD3 ϵ WT, F.CD3 ϵ K76T, and F.CD3 ϵ C80G cells were stimulated for 7 hr with 3 μ g/ml plate-bound 2C11 followed by staining the cells with anti-CD69 and gating on the GFP $^{+}$ cells for analysis by flow cytometry (n = 3). The mean \pm SD is shown. One-way ANOVA and post hoc Tukey HSD tests were used: ***p < 0.001. (B) The V γ 9V δ 2 T cell clone was stimulated in triplicates for 4 (CD69) or 20 (CD25) hr with 5 μ g/ml soluble UCHT1 or OKT3 and stained with anti-CD69 or anti-CD25 for flow cytometry (n > 3). (C) Human freshly isolated, purified $\gamma\delta$ T cells ($\gamma\delta$ PBMCs) were stimulated for 20 hr and analyzed as in (B) (n = 1). (D) The cellular supernatants from (B, 4 hr) were used to measure IFN- γ and TNF- α by a multiplexed bead assay (IFN- γ n = 2, TNF- α n = 3). (E) The V γ 9V δ 2 T cell clone was stimulated with 5 μ g/ml plate-bound UCHT1 or OKT3 in triplicates and secreted IFN- γ and TNF- α were quantified as above (n = 2). (F) Expanded primary blood $\gamma\delta$ T cells were labeled with 1 μ M Cell Trace Violet and left unstimulated or stimulated with 5 μ g/ml soluble UCHT1 or OKT3 as indicated. After 4 days, proliferation was determined by flow cytometry (left panel) (n = 3). In (B)–(E), mean \pm SD of triplicates is shown. Significances between UCHT1- and OKT3-stimulated cells were determined by the Student's t test; ns, not significant; *p < 0.05; **p < 0.01; ***p < 0.001.

$\alpha\beta$ TCR (de la Cruz et al., 2011; Gil et al., 2008). Therefore, the $\gamma\delta$ TCRs tested do not undergo the CD3 CC upon engagement by their ligands, which is in sharp contrast to the $\alpha\beta$ TCR (Figure S7A).

In neither $\alpha\beta$ nor $\gamma\delta$ TCRs was exposure of the PRS influenced by the presence or absence of Ca $^{2+}$ ions. This indicates that the CD3 CC is different from the proposed Ca $^{2+}$ -dependent detachment of the CD3 ϵ cytoplasmic tail from the membrane (Shi et al., 2013), and most likely it occurs upstream of TCR-induced Ca $^{2+}$ signaling. Likewise, the absence of the CD3 ϵ basic-rich sequence, required for membrane binding of the CD3 ϵ tail, did not influence the CD3 CC (de la Cruz et al., 2011).

What might be the difference between $\gamma\delta$ TCRs and $\alpha\beta$ TCRs that precludes the CD3 CC upon antigen stimulation of the $\gamma\delta$ TCR? First, a low antigen- $\gamma\delta$ TCR affinity can be excluded, because the T22-G8 TCR $\gamma\delta$ interaction is high affinity K $_D$ \approx 100 nM (Crowley et al., 2000), compared to \approx 10 μ M for typical pMHC-TCR $\alpha\beta$ interactions (Davis et al., 1998). Second, using chimeric TCRs, we observed that induction of the CD3 CC did not depend on pMHC versus T22 binding, but on the C regions of the TCR $\alpha\beta$ heterodimer. Thus, it is unlikely that the differential geometry of the T22- $\gamma\delta$ TCR interaction compared to the pMHC- $\alpha\beta$ TCR interaction (Adams et al., 2005; Rudolph

et al., 2006) is the cause for the absence of this structural change in the $\gamma\delta$ TCR.

The capacity to undergo the CD3 CC (or not) mapped to the C regions of TCR $\gamma\delta$ /TCR $\alpha\beta$. In fact, the constant Ig domains of TCR $\gamma\delta$ use different amino acids to associate with CD3 than do those of the TCR $\alpha\beta$ (Allison et al., 2001), which is in line with previous data suggesting that TCR $\alpha\beta$ are oriented differently toward CD3 compared to TCR $\gamma\delta$ (Van Neerven et al., 1990). For example, the constant Ig domain of TCR β contains an FG loop that is thought to directly associate with CD3 (Touma et al., 2006) and that is not present in TCR $\gamma\delta$. The structural difference might be subtle, because in both TCR types the CD3 dimers might be located on the same side (Kuhns et al., 2010). Thus, our data suggest that the arrangement of the complete TCR $\gamma\delta$ -CD3- ζ complex might sterically hinder antigen-induced conversion into the open CD3 conformation. In contrast to antigens, anti-TCR mAbs can force the $\gamma\delta$ TCR to adopt the CD3 open conformation. Thus, it is possible that some $\gamma\delta$ TCRs could undergo the CD3 CC upon binding to their ligand.

Despite the fact that the anti-human CD3 mAbs UCHT1 and OKT3 recognize overlapping epitopes at CD3 ϵ (Arnett et al., 2004; Kjer-Nielsen et al., 2004), UCHT1 induced the CD3 CC in

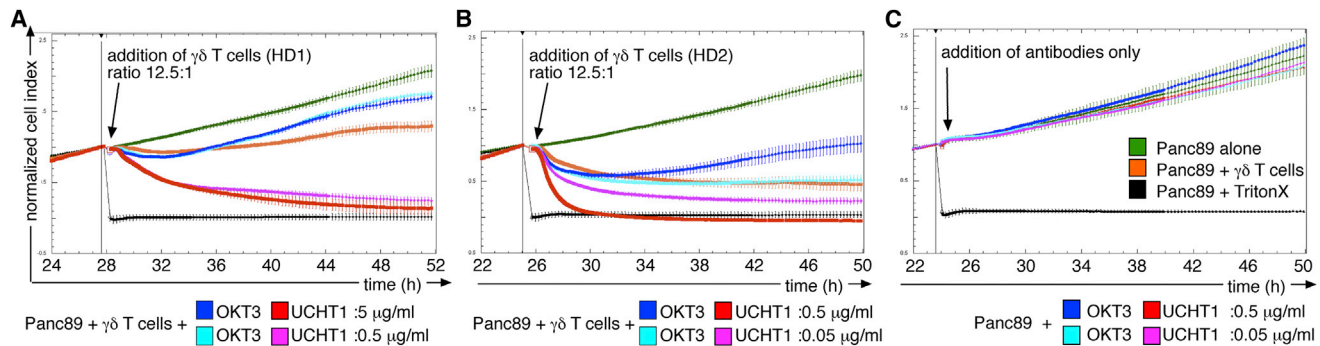


Figure 7. UCHT1, but Not OKT3, Enhances $V\gamma 9V\delta 2$ T Cell-Mediated Tumor Cell Lysis

(A and B) Adherent pancreatic ductal adenocarcinoma Panc89 cells were grown on an E-plate of a Real Time Cell Analyzer. After 24 hr human short-term cultured $V\gamma 9V\delta 2$ T cell lines from healthy donor (HD) 1 (A) or HD2 (B) in medium (orange) or together with the indicated concentrations of the mAbs UCHT1 or OKT3 were added to the assay. The effector target ratio was 12.5:1. The cell index was determined every 5 min over the course of the experiment and normalized to 1 at the time point of addition of antibodies and $\gamma\delta$ T cells as shown by the vertical black thin line. The loss of impedance (corresponding to induction of tumor cell lysis) after addition of the $\gamma\delta$ T cells was measured over additional 24 hr. Growth of the tumor cells alone (green) or lysis by detergent (black) are shown as controls. Results of two representative donors out of seven are shown.

(C) The experiment was performed as in (B), but without adding $\gamma\delta$ T cells.

the $\gamma\delta$ TCR, whereas OKT3 did not. This was intrinsic to the $\gamma\delta$ TCR. In contrast, both mAbs triggered the CD3 CC in the $\alpha\beta$ TCR. OKT3 therefore resembles the T22 ligand in the murine system. Thus, mAbs can be useful tools for studying the TCR but do not always mimic antigen engagement. The $\gamma\delta$ TCR is more extensively glycosylated on CD3 compared to the $\alpha\beta$ TCR (Aларcon et al., 1987; Krangel et al., 1987; Siegers et al., 2007; Van Neerven et al., 1990). Indeed, we show that desialylation of $\gamma\delta$ T cells enabled OKT3 to induce the CD3 CC in the $V\gamma 9V\delta 2$ TCR. This $\gamma\delta$ -specific CD3 glycosylation was dependent on the expression of TCR $\gamma\delta$ and not the cellular background (Siegers et al., 2007), which correlates with the inability of OKT3 to induce the CD3 CC in Jk. $V\gamma 9V\delta 2$ T cells. CD3 deglycosylation (or deglycosylation of other cell surface proteins) might also enhance $\gamma\delta$ TCR clustering, promoting the CD3 CC.

In $\alpha\beta$ T cells, the CD3 CC was required for $\alpha\beta$ TCR triggering (Martínez-Martín et al., 2009; Minguet and Schamel, 2008). We observed activation of human $V\gamma 9V\delta 2$ T cells and murine G8 $\gamma\delta$ T cells by antigen in the absence of detectable induction of the CD3 CC (Figure S7A). Furthermore, mutating CD3 ϵ such that its capacity to undergo the CD3 CC was reduced (Martínez-Martín et al., 2009) did not impair upregulation of the activation marker CD69 in murine $V\gamma 1.1$ T cells. Thus, in contrast to $\alpha\beta$ TCRs, the three different $\gamma\delta$ TCRs tested did not require the CD3 CC for several T cell activation readouts. Perhaps the absence of CD3 CC at the $\gamma\delta$ TCR is compensated by higher kinase levels (Laird and Hayes, 2010), expression of different kinases (Latour et al., 1997; Saint-Ruf et al., 2000), or a higher capacity to cluster (Jensen et al., 2008). Indeed, $\gamma\delta$ T cells have an intrinsically stronger signaling capacity (Haks et al., 2005; Hayes et al., 2005) and may not need the CD3 CC to amplify activation signals as $\alpha\beta$ T cells do.

Artificial induction of the CD3 CC in the human $V\gamma 9V\delta 2$ TCR by stimulation with UCHT1 had a strong impact on $\gamma\delta$ T cell activation. Compared to OKT3, UCHT1 stimulation enhanced proximal $\gamma\delta$ TCR-induced signaling events, such as Ca^{2+} influx and activation of the PI3K/AKT, Ras/Erk and $I\kappa B$ /NF κB pathways

(Figure S7B). Complementing OKT3 with the CD3 CC by T cell desialylation, anti- κ light chain or anti-igG treatment resulted in augmented proximal signaling, suggesting that the CD3 CC was the cause for this increased activation. Indeed, Ca^{2+} influx was reduced in the CD3 CC-defective mutant murine $\gamma\delta$ TCRs. This is in line with $\alpha\beta$ T cells, in which the CD3 CC is required for proximal signaling (Martínez-Martín et al., 2009; Minguet and Schamel, 2008). Furthermore, the lack of CD3 CC during $\gamma\delta$ TCR triggering explains the slow kinetics (in comparison to those of $\alpha\beta$ T cells) and weak intensities of proximal signaling when human $V\gamma 9V\delta 2$ T cells were stimulated with phosphoantigens and OKT3 (Beetz et al., 2008; Correia et al., 2009; Lafont et al., 2001), but not with UCHT1 (Lafont et al., 2001).

In contrast to proximal signaling events, production of the effector cytokine IFN- γ and TNF- α by the $V\gamma 9V\delta 2$ cells was reduced when the CD3 CC was present. It seems likely that strong proximal signaling supported by the CD3 CC (UCHT1) activates negative feedback loops, which decreases signaling at later time points. Indeed, UCHT1 enhanced TCR downregulation compared to OKT3. Thus, the lack of negative feedback loops upon OKT3 stimulation might explain the heightened ability of OKT3 to trigger cytokine production. Indeed, $\gamma\delta$ T cells are strong cytokine producers (Bonneville et al., 2010; Chien and Königshofer, 2007; Vantourout and Hayday, 2013).

Immunotherapy using $\gamma\delta$ T cells is garnering ever-increasing interest and has been tested in several early phase clinical trials for different cancers (Bennouna et al., 2008; Dieli et al., 2007; Kobayashi et al., 2007; Wilhelm et al., 2003; Xu et al., 2008). $\gamma\delta$ T cells may be expanded in vivo (Dieli et al., 2007) or ex vivo and adoptively transferred (Bennouna et al., 2008; Kobayashi et al., 2011; Nicol et al., 2011). In fact, allogeneic transplantation is now being considered a doable option, because $\gamma\delta$ T cells do not incite graft-versus-host disease, while offering considerable graft-versus-malignancy effects (Daniele et al., 2012). One limiting factor is that patient-derived $\gamma\delta$ T cells, especially from those who have received chemotherapy or prior zoledronate treatment, often undergo suboptimal and highly variable

ex vivo expansion (Kobayashi et al., 2011; Nicol et al., 2011). We show here that OKT3 stimulation, which does not induce the CD3 CC at the $\gamma\delta$ TCR, promotes strong proliferation. Thus, it may be ideally suited for the expansion of $\gamma\delta$ T cells and was used for this purpose before (Dokouhaki et al., 2010).

Besides cellular expansion strong $\gamma\delta$ T cell activation might be also required for therapeutic efficacy (Pennington et al., 2005). We found that induction of the CD3 CC enhanced the PI3K/Akt and Ras/Erk pathways that are necessary for the antitumor activity of V γ 9V δ 2 T cells (Correia et al., 2009). Thus, UCHT1, which induces the CD3 CC, strongly enhanced $\gamma\delta$ T cell-mediated tumor cell killing, resulting in death of all tumor cells. In sharp contrast, OKT3 slightly blocked the tumor killing activity of the V γ 9V δ 2 T cells in most experiments. This was neither due to enhanced $\gamma\delta$ T cell proliferation nor increased IFN- γ or TNF- α production by UCHT1-stimulated cells, because OKT3 triggered greater proliferation as well as IFN- γ and TNF- α production than UCHT1. UCHT1 and OKT3 also induced similar amounts of apoptosis in the $\gamma\delta$ T cells. The conclusion that the CD3 CC promotes $\gamma\delta$ T cell cytotoxicity could be confirmed by genetic means using the CD3 CC mutant CD3 ϵ in the tumor-killing assay.

Thus, employing these two mAbs may constitute an ideal combination in the development of $\gamma\delta$ T cell immunotherapy for a variety of cancers. Phosphoantigen stimulation at culture initiation followed by OKT3 stimulation should ensure generation of sufficient $\gamma\delta$ T cell numbers for infusion (Dokouhaki et al., 2010; Lopez et al., 2000) and UCHT1 stimulation just prior to infusion would enhance cytotoxicity.

In summary, our study identifies fundamental differences in $\gamma\delta$ TCR versus $\alpha\beta$ TCR triggering mechanisms, which have likely evolved in response to differences in the respective antigens recognized by these receptors. Our findings, suggesting the use of UCHT1 or other drugs inducing the CD3 CC in human $\gamma\delta$ T cells, may inform the design of novel clinical immunotherapy protocols.

EXPERIMENTAL PROCEDURES

Cells, Mice, Reagents, and Cloning

This information is given in the Supplemental Information.

Cell Stimulation, Lysis, and Nck-PD Assay

Cells were stimulated for 5 min or the indicated times at 37°C or for 30 min on ice with 5 μ g/ml anti-TCR. Cells were lysed at a maximum of 30×10^6 cells/ml in 1 ml lysis buffer containing the indicated detergent (0.3% Brij96V or 0.3% Brij58) as described (Schamel et al., 2005). Fifty microliters were kept as a lysate control. For the SH3-PD assay, 600 μ l were incubated with 3–5 μ l glutathione-Sepharose beads bound to the first SH3 domain of Nck for 3 hr at 4°C (Gil et al., 2002). Beads were washed vigorously four times in lysis buffer containing 0.5% Brij96V. Three hundred microliters of the lysate was used to confirm antibody binding of the stimulating antibodies by immunoprecipitations using 3 μ l protein G- and 3 μ l protein A-coupled Sepharose (Amersham Pharmacia Biotech) as described (Schamel et al., 2005).

T1.4 $\alpha\beta$ hybridoma cells were incubated with photoreactive H2-K^d-pepABA monomers or tetramers. Subsequently, cells were UV-irradiated to covalently crosslink the pMHC to the T1.4 $\alpha\beta$ TCR. Upon lysis, the SH3-PD was performed as above.

For stimulation by APCs, we used splenic B cells from CD3 ϵ knock out C57BL/6 mice (avoiding contamination by T cells) that were stimulated overnight with 5 μ g/ml LPS, Daudi cells, or Daudi cells pulsed for 4 hr with 2 μ M zoledronate 10 hr before use. T cells were mixed with the APCs at a 1:1 ($\gamma\delta$

T cell:Daudi cell) or 1:2 (G8 $\gamma\delta$ T cell hybridoma:splenic APC) ratio. After stimulation and lysis, the SH3-PD was performed as above. For the unstimulated cells, T cells and APCs were lysed separately, and the lysates were combined for the SH3-PD.

Activation Assays

For the measurement of phosphorylated Erk, Akt, and I κ B α , cells were stimulated and lysed and a multiplexed bead assay was performed using BioPlex200 system as per the manufacturer's instruction (Bio-Rad). To induce TCR downmodulation or CD69 and CD25 upregulation cells were plated at 2×10^5 per 96-well plate well and soluble antibodies were added at a concentration of 5 μ g/ml. Cells were incubated at 37°C as indicated. Supernatants were kept at –80°C, and the relative amount of IFN- γ and TNF- α was measured within 2 weeks on the BioPlex200 system following the manufacturer's instruction (Bio-Rad). Alternatively, TNF- α was measured using an ELISA kit (BD Biosciences).

Ca²⁺ Flux and Flow Cytometry

Cells were labeled in the dark with 5 μ g/ml of Indo-1 and 0.5 μ g/ml of pluronic F-127 (both Molecular Probes and Life Technologies) for 45 min in RPMI, 1% fetal calf serum. After 1 min of recording at 37°C, cells were stimulated with 5 μ g/ml OKT3 or UCHT1 mAb with or without 2.5 μ g/ml of the indicated cross-linking antibody. The change of the ratio of Indo-bound versus Indo-unbound was followed for 300 s with a LSRII fluorescence spectrometer (BD Biosciences). Data were analyzed with the FlowJo 6.1 software.

Tumor Cell Killing Assay

Adherent pancreatic ductal adenocarcinoma Panc89 cells were added to wells of an E-plate of a Real Time Cell Analyzer (Roche) for 24 hr. The impedance of the tumor cells was measured over this time period. After 24 hr, when the tumor cells were in the linear growth phase, the indicated concentrations of anti-CD3 mAb or medium together with the short-term cultured $\gamma\delta$ T cell lines were added. The loss of impedance after addition of $\gamma\delta$ T cells was measured over additional 24 hr. As a control for maximal lysis, Triton X-100 was added to the Panc89 cells.

SUPPLEMENTAL INFORMATION

Supplemental Information includes Supplemental Experimental Procedures and seven figures and can be found with this article online at <http://dx.doi.org/10.1016/j.celrep.2014.04.049>.

AUTHOR CONTRIBUTIONS

E.P.D., F.A.H., H.-H.O., G.M.S., O.S.Y., S.K., G.J.F., and B.G. designed some and performed all experiments. J.R.R., D.K., S.M., D.W., P.F., and W.W.A.S. designed most of the experiments. A.S. and E.J.A. prepared the T22 monomers and BA provided the CD3 ϵ mutants. W.W.A.S. conceived the project. E.P.D., D.K., G.M.S., S.M., D.W., and W.W.A.S. wrote and edited the manuscript.

ACKNOWLEDGMENTS

This work was supported by the German Research Foundation (DFG) through grants SFB620 to W.W.A.S. and P.F., SCHA976/2-1 to W.W.A.S., the Excellence Initiatives GSC-4 (Spemann Graduate School), EXC294 (BIOSS) to G.J.F. and W.W.A.S., EXC306 (Inflammation-at-Interfaces) to D.K., the Pancreatic Cancer Consortium Kiel (WE 3559/2-1) to D.W. and D.K., the EU through grant FP7/2007-2013 (SYBILLA) to W.W.A.S., E.P.D., and B.A., the Innovation-fonds Forschung-2012 grant to F.A.H. and S.M., MEC (SAF2011-24235) to B.G., and the Fundacion Ramon Areces to B.A. We much appreciate Y.H. Chien, G. DeLiberio, C. Belmant, E. Champagne, H. Kalthoff, I. Lüscher, and the BIOSS toolbox for providing us with reagents and discussions.

Received: May 18, 2013

Revised: March 15, 2014

Accepted: April 23, 2014

Published: May 22, 2014

REFERENCES

- Adams, E.J., Chien, Y.H., and Garcia, K.C. (2005). Structure of a gammadelta T cell receptor in complex with the nonclassical MHC T22. *Science* *308*, 227–231.
- Adams, E.J., Strop, P., Shin, S., Chien, Y.H., and Garcia, K.C. (2008). An autonomous CDR3 δ is sufficient for recognition of the nonclassical MHC class I molecules T10 and T22 by gammadelta T cells. *Nat. Immunol.* *9*, 777–784.
- Alarcon, B., De Vries, J., Pettey, C., Boylston, A., Yssel, H., Terhorst, C., and Spits, H. (1987). The T-cell receptor gamma chain-CD3 complex: implication in the cytotoxic activity of a CD3+ CD4- CD8- human natural killer clone. *Proc. Natl. Acad. Sci. USA* *84*, 3861–3865.
- Alibaud, L., Arnaud, J., Llobera, R., and Rubin, B. (2001). On the role of CD3 δ chains in TCRgammadelta/CD3 complexes during assembly and membrane expression. *Scand. J. Immunol.* *54*, 155–162.
- Allison, T.J., Winter, C.C., Fournié, J.J., Bonneville, M., and Garboczi, D.N. (2001). Structure of a human gammadelta T-cell antigen receptor. *Nature* *411*, 820–824.
- Amett, K.L., Harrison, S.C., and Wiley, D.C. (2004). Crystal structure of a human CD3- ϵ/δ dimer in complex with a UCHT1 single-chain antibody fragment. *Proc. Natl. Acad. Sci. USA* *101*, 16268–16273.
- Beetz, S., Wesch, D., Marischen, L., Welte, S., Oberg, H.H., and Kabelitz, D. (2008). Innate immune functions of human gammadelta T cells. *Immunobiology* *213*, 173–182.
- Bennouna, J., Bompas, E., Neidhardt, E.M., Rolland, F., Philip, I., Galéa, C., Salot, S., Saiagh, S., Audrain, M., Rimbart, M., et al. (2008). Phase-I study of Innacell gammadelta, an autologous cell-therapy product highly enriched in $\gamma 9\delta 2$ T lymphocytes, in combination with IL-2, in patients with metastatic renal cell carcinoma. *Cancer Immunol. Immunother.* *57*, 1599–1609.
- Bluestone, J.A., Cron, R.Q., Cotterman, M., Houlden, B.A., and Matis, L.A. (1988). Structure and specificity of T cell receptor γ/δ on major histocompatibility complex antigen-specific CD3+, CD4-, CD8- T lymphocytes. *J. Exp. Med.* *168*, 1899–1916.
- Bonneville, M., O'Brien, R.L., and Born, W.K. (2010). Gammadelta T cell effector functions: a blend of innate programming and acquired plasticity. *Nat. Rev. Immunol.* *10*, 467–478.
- Borroto, A., Arellano, I., Dopfer, E.P., Prouza, M., Suchànek, M., Fuentes, M., Orfao, A., Schamel, W.W., and Alarcón, B. (2013). Nck recruitment to the TCR required for ZAP70 activation during thymic development. *J. Immunol.* *190*, 1103–1112.
- Borroto, A., Arellano, I., Blanco, R., Fuentes, M., Orfao, A., Dopfer, E.P., Prouza, M., Suchànek, M., Schamel, W.W., and Alarcón, B. (2014). Relevance of Nck-CD3 epsilon interaction for T cell activation in vivo. *J. Immunol.* *192*, 2042–2053.
- Bukowski, J.F., Morita, C.T., Tanaka, Y., Bloom, B.R., Brenner, M.B., and Band, H. (1995). V $\gamma 2\delta 2$ TCR-dependent recognition of non-peptide antigens and Daudi cells analyzed by TCR gene transfer. *J. Immunol.* *154*, 998–1006.
- Bukowski, J.F., Morita, C.T., Band, H., and Brenner, M.B. (1998). Crucial role of TCR γ chain junctional region in prenyl pyrophosphate antigen recognition by $\gamma\delta$ T cells. *J. Immunol.* *161*, 286–293.
- Chien, Y.H., and Konigshofer, Y. (2007). Antigen recognition by gammadelta T cells. *Immunol. Rev.* *215*, 46–58.
- Constant, P., Davodeau, F., Peyrat, M.A., Poquet, Y., Puzo, G., Bonneville, M., and Fournié, J.J. (1994). Stimulation of human $\gamma\delta$ T cells by nonpeptidic mycobacterial ligands. *Science* *264*, 267–270.
- Correia, D.V., d'Orey, F., Cardoso, B.A., Lança, T., Grosso, A.R., deBarros, A., Martins, L.R., Barata, J.T., and Silva-Santos, B. (2009). Highly active microbial phosphoantigen induces rapid yet sustained MEK/Erk- and PI-3K/Akt-mediated signal transduction in anti-tumor human gammadelta T-cells. *PLoS ONE* *4*, e5657.
- Crowley, M.P., Fahrner, A.M., Baumgarth, N., Hampl, J., Gutgemann, I., Teyton, L., and Chien, Y. (2000). A population of murine gammadelta T cells that recognize an inducible MHC class Ib molecule. *Science* *287*, 314–316.
- Daniele, N., Scerpa, M.C., Caniglia, M., Bernardo, M.E., Rossi, C., Ciammetti, C., Palumbo, G., Locatelli, F., Isacchi, G., and Zinno, F. (2012). Transplantation in the onco-hematology field: focus on the manipulation of $\alpha\beta$ and $\gamma\delta$ T cells. *Pathol. Res. Pract.* *208*, 67–73.
- Davis, M.M., Boniface, J.J., Reich, Z., Lyons, D., Hampl, J., Arden, B., and Chien, Y. (1998). Ligand recognition by $\alpha\beta$ T cell receptors. *Annu. Rev. Immunol.* *16*, 523–544.
- de la Cruz, J., Kruger, T., Parks, C.A., Silge, R.L., van Oers, N.S., Luescher, I.F., Schrum, A.G., and Gil, D. (2011). Basal and antigen-induced exposure of the proline-rich sequence in CD3 ϵ . *J. Immunol.* *186*, 2282–2290.
- Deford-Watts, L.M., Tassin, T.C., Becker, A.M., Medeiros, J.J., Albanesi, J.P., Love, P.E., Wülfing, C., and van Oers, N.S. (2009). The cytoplasmic tail of the T cell receptor CD3 ϵ subunit contains a phospholipid-binding motif that regulates T cell functions. *J. Immunol.* *183*, 1055–1064.
- Dieli, F., Vermijlen, D., Fulfaro, F., Caccamo, N., Meraviglia, S., Cicero, G., Roberts, A., Buccheri, S., D'Asaro, M., Gebbia, N., et al. (2007). Targeting human $\gamma\delta$ T cells with zoledronate and interleukin-2 for immunotherapy of hormone-refractory prostate cancer. *Cancer Res.* *67*, 7450–7457.
- Dokouhaki, P., Han, M., Joe, B., Li, M., Johnston, M.R., Tsao, M.S., and Zhang, L. (2010). Adoptive immunotherapy of cancer using ex vivo expanded human gammadelta T cells: A new approach. *Cancer Lett.* *297*, 126–136.
- Espinosa, E., Belmont, C., Pont, F., Luciani, B., Poupot, R., Romagné, F., Brailly, H., Bonneville, M., and Fournié, J.J. (2001). Chemical synthesis and biological activity of bromohydrin pyrophosphate, a potent stimulator of human $\gamma\delta$ T cells. *J. Biol. Chem.* *276*, 18337–18344.
- Fisch, P., Malkovsky, M., Braakman, E., Sturm, E., Bolhuis, R.L., Prieve, A., Sosman, J.A., Lam, V.A., and Sondel, P.M. (1990a). γ/δ T cell clones and natural killer cell clones mediate distinct patterns of non-major histocompatibility complex-restricted cytotoxicity. *J. Exp. Med.* *171*, 1567–1579.
- Fisch, P., Malkovsky, M., Kovats, S., Sturm, E., Braakman, E., Klein, B.S., Voss, S.D., Morrissey, L.W., DeMars, R., Welch, W.J., et al. (1990b). Recognition by human V $\gamma 9/V \delta 2$ T cells of a GroEL homolog on Daudi Burkitt's lymphoma cells. *Science* *250*, 1269–1273.
- Fisch, P., Meuer, E., Pende, D., Rothenfusser, S., Viale, O., Kock, S., Ferrone, S., Fradelizi, D., Klein, G., Moretta, L., et al. (1997). Control of B cell lymphoma recognition via natural killer inhibitory receptors implies a role for human Vgamma9/Vdelta2 T cells in tumor immunity. *Eur. J. Immunol.* *27*, 3368–3379.
- Gil, D., Schamel, W.W., Montoya, M., Sánchez-Madrid, F., and Alarcón, B. (2002). Recruitment of Nck by CD3 epsilon reveals a ligand-induced conformational change essential for T cell receptor signaling and synapse formation. *Cell* *109*, 901–912.
- Gil, D., Schrum, A.G., Alarcón, B., and Palmer, E. (2005). T cell receptor engagement by peptide-MHC ligands induces a conformational change in the CD3 complex of thymocytes. *J. Exp. Med.* *201*, 517–522.
- Gil, D., Schrum, A.G., Daniels, M.A., and Palmer, E. (2008). A role for CD8 in the developmental tuning of antigen recognition and CD3 conformational change. *J. Immunol.* *180*, 3900–3909.
- Gober, H.J., Kistowska, M., Angman, L., Jenö, P., Mori, L., and De Libero, G. (2003). Human T cell receptor gammadelta cells recognize endogenous mevalonate metabolites in tumor cells. *J. Exp. Med.* *197*, 163–168.
- Haks, M.C., Lefebvre, J.M., Lauritsen, J.P., Carleton, M., Rhodes, M., Miyazaki, T., Kappes, D.J., and Wiest, D.L. (2005). Attenuation of gammadeltaTCR signaling efficiently diverts thymocytes to the alphabeta lineage. *Immunity* *22*, 595–606.
- Hayes, S.M., Li, L., and Love, P.E. (2005). TCR signal strength influences alphabeta/gammadelta lineage fate. *Immunity* *22*, 583–593.
- Janssen, O., Wesselborg, S., Heckl-Ostreicher, B., Pechhold, K., Bender, A., Schondelmaier, S., Moldenhauer, G., and Kabelitz, D. (1991). T cell receptor/CD3-signaling induces death by apoptosis in human T cell receptor $\gamma\delta$ + T cells. *J. Immunol.* *146*, 35–39.

- Jensen, K.D., Su, X., Shin, S., Li, L., Youssef, S., Yamasaki, S., Steinman, L., Saito, T., Locksley, R.M., Davis, M.M., et al. (2008). Thymic selection determines gammadelta T cell effector fate: antigen-naive cells make interleukin-17 and antigen-experienced cells make interferon γ . *Immunity* 29, 90–100.
- Kabelitz, D., Ackermann, T., Hinz, T., Davodeau, F., Band, H., Bonneville, M., Janssen, O., Arden, B., and Schondelmaier, S. (1994). New monoclonal antibody (23D12) recognizing three different V γ elements of the human $\gamma\delta$ T cell receptor. 23D12+ cells comprise a major subpopulation of $\gamma\delta$ T cells in post-natal thymus. *J. Immunol.* 152, 3128–3136.
- Kjer-Nielsen, L., Dunstone, M.A., Kostenko, L., Ely, L.K., Beddoe, T., Mifsud, N.A., Purcell, A.W., Brooks, A.G., McCluskey, J., and Rossjohn, J. (2004). Crystal structure of the human T cell receptor CD3 epsilon gamma heterodimer complexed to the therapeutic mAb OKT3. *Proc. Natl. Acad. Sci. USA* 101, 7675–7680.
- Kobayashi, H., Tanaka, Y., Yagi, J., Osaka, Y., Nakazawa, H., Uchiyama, T., Minato, N., and Toma, H. (2007). Safety profile and anti-tumor effects of adoptive immunotherapy using $\gamma\delta$ T cells against advanced renal cell carcinoma: a pilot study. *Cancer Immunol. Immunother.* 56, 469–476.
- Kobayashi, H., Tanaka, Y., Yagi, J., Minato, N., and Tanabe, K. (2011). Phase I/II study of adoptive transfer of $\gamma\delta$ T cells in combination with zoledronic acid and IL-2 to patients with advanced renal cell carcinoma. *Cancer Immunol. Immunother.* 60, 1075–1084.
- Krangel, M.S., Bierer, B.E., Devlin, P., Clabby, M., Strominger, J.L., McLean, J., and Brenner, M.B. (1987). T3 glycoprotein is functional although structurally distinct on human T-cell receptor γ T lymphocytes. *Proc. Natl. Acad. Sci. USA* 84, 3817–3821.
- Kuhns, M.S., and Davis, M.M. (2012). TCR signaling emerges from the sum of many parts. *Front Immunol* 3, 159.
- Kuhns, M.S., Girvin, A.T., Klein, L.O., Chen, R., Jensen, K.D., Newell, E.W., Huppa, J.B., Lillemeier, B.F., Huse, M., Chien, Y.H., et al. (2010). Evidence for a functional sidedness to the alphabetaTCR. *Proc. Natl. Acad. Sci. USA* 107, 5094–5099.
- Lafont, V., Liautaud, J., Sable-Teychene, M., Sainte-Marie, Y., and Favero, J. (2001). Isopentenyl pyrophosphate, a mycobacterial non-peptidic antigen, triggers delayed and highly sustained signaling in human $\gamma\delta$ T lymphocytes without inducing down-modulation of T cell antigen receptor. *J. Biol. Chem.* 276, 15961–15967.
- Laird, R.M., and Hayes, S.M. (2010). Roles of the Src tyrosine kinases Lck and Fyn in regulating gammadeltaTCR signal strength. *PLoS ONE* 5, e8899.
- Latour, S., Fournel, M., and Veillette, A. (1997). Regulation of T-cell antigen receptor signalling by Syk tyrosine protein kinase. *Mol. Cell. Biol.* 17, 4434–4441.
- Lopez, R.D., Xu, S., Guo, B., Negrin, R.S., and Waller, E.K. (2000). CD2-mediated IL-12-dependent signals render human $\gamma\delta$ T cells resistant to mitogen-induced apoptosis, permitting the large-scale ex vivo expansion of functionally distinct lymphocytes: implications for the development of adoptive immunotherapy strategies. *Blood* 96, 3827–3837.
- Martínez-Martín, N., Risueño, R.M., Morreale, A., Zaldívar, I., Fernández-Arenas, E., Herranz, F., Ortiz, A.R., and Alarcón, B. (2009). Cooperativity between T cell receptor complexes revealed by conformational mutants of CD3epsilon. *Sci. Signal.* 2, ra43.
- Matis, L.A., Cron, R., and Bluestone, J.A. (1987). Major histocompatibility complex-linked specificity of $\gamma\delta$ receptor-bearing T lymphocytes. *Nature* 330, 262–264.
- Minguet, S., and Schamel, W.W. (2008). A permissive geometry model for TCR-CD3 activation. *Trends Biochem. Sci.* 33, 51–57.
- Minguet, S., Swamy, M., Alarcón, B., Luescher, I.F., and Schamel, W.W. (2007). Full activation of the T cell receptor requires both clustering and conformational changes at CD3. *Immunity* 26, 43–54.
- Nicol, A.J., Tokuyama, H., Mattarollo, S.R., Hagi, T., Suzuki, K., Yokokawa, K., and Nieda, M. (2011). Clinical evaluation of autologous $\gamma\delta$ T cell-based immunotherapy for metastatic solid tumours. *Br. J. Cancer* 105, 778–786.
- Pennington, D.J., Vermijlen, D., Wise, E.L., Clarke, S.L., Tigelaar, R.E., and Hayday, A.C. (2005). The integration of conventional and unconventional T cells that characterizes cell-mediated responses. *Adv. Immunol.* 87, 27–59.
- Risueño, R.M., Gil, D., Fernández, E., Sánchez-Madrid, F., and Alarcón, B. (2005). Ligand-induced conformational change in the T-cell receptor associated with productive immune synapses. *Blood* 106, 601–608.
- Risueño, R.M., van Santen, H.M., and Alarcón, B. (2006). A conformational change senses the strength of T cell receptor-ligand interaction during thymic selection. *Proc. Natl. Acad. Sci. USA* 103, 9625–9630.
- Risueño, R.M., Schamel, W.W., and Alarcón, B. (2008). T cell receptor engagement triggers its CD3e and CD3z subunits to adopt a compact, locked conformation. *PLoS One* 3, e1747.
- Roelofs, A.J., Jauhainen, M., Mönkkönen, H., Rogers, M.J., Mönkkönen, J., and Thompson, K. (2009). Peripheral blood monocytes are responsible for gammadelta T cell activation induced by zoledronic acid through accumulation of IPP/DMAPP. *Br. J. Haematol.* 144, 245–250.
- Rudolph, M.G., Stanfield, R.L., and Wilson, I.A. (2006). How TCRs bind MHCs, peptides, and coreceptors. *Annu. Rev. Immunol.* 24, 419–466.
- Saint-Ruf, C., Panigada, M., Azogui, O., Debey, P., von Boehmer, H., and Grassi, F. (2000). Different initiation of pre-TCR and gammadeltaTCR signalling. *Nature* 406, 524–527.
- Schamel, W.W., Arechaga, I., Risueño, R.M., van Santen, H.M., Cabezas, P., Risco, C., Valpuesta, J.M., and Alarcón, B. (2005). Coexistence of multivalent and monovalent TCRs explains high sensitivity and wide range of response. *J. Exp. Med.* 202, 493–503.
- Schild, H., Mavaddat, N., Litzenberger, C., Ehrlich, E.W., Davis, M.M., Bluestone, J.A., Matis, L., Draper, R.K., and Chien, Y.H. (1994). The nature of major histocompatibility complex recognition by $\gamma\delta$ T cells. *Cell* 76, 29–37.
- Shi, X., Bi, Y., Yang, W., Guo, X., Jiang, Y., Wan, C., Li, L., Bai, Y., Guo, J., Wang, Y., et al. (2013). Ca²⁺ regulates T-cell receptor activation by modulating the charge property of lipids. *Nature* 493, 111–115.
- Siegers, G.M., Swamy, M., Fernández-Malavé, E., Minguet, S., Rathmann, S., Guardo, A.C., Pérez-Flores, V., Regueiro, J.R., Alarcón, B., Fisch, P., and Schamel, W.W. (2007). Different composition of the human and the mouse gammadelta T cell receptor explains different phenotypes of CD3 γ and CD3 δ immunodeficiencies. *J. Exp. Med.* 204, 2537–2544.
- Spaner, D., Cohen, B.L., Miller, R.G., and Phillips, R.A. (1995). Antigen-presenting cells for naive transgenic $\gamma\delta$ T cells. Potent activation by activated $\alpha\beta$ T cells. *J. Immunol.* 155, 3866–3876.
- Tanaka, Y., Morita, C.T., Tanaka, Y., Nieves, E., Brenner, M.B., and Bloom, B.R. (1995). Natural and synthetic non-peptide antigens recognized by human $\gamma\delta$ T cells. *Nature* 375, 155–158.
- Touma, M., Chang, H.C., Sasada, T., Handley, M., Clayton, L.K., and Reinherz, E.L. (2006). The TCR C β FG loop regulates $\alpha\beta$ T cell development. *J. Immunol.* 176, 6812–6823.
- Van Neerven, J., Coligan, J.E., and Koning, F. (1990). Structural comparison of $\alpha\beta$ and $\gamma\delta$ T cell receptor-CD3 complexes reveals identical subunit interactions but distinct cross-linking patterns of T cell receptor chains. *Eur. J. Immunol.* 20, 2105–2111.
- Vantourout, P., and Hayday, A. (2013). Six-of-the-best: unique contributions of $\gamma\delta$ T cells to immunology. *Nat. Rev. Immunol.* 13, 88–100.
- Weintraub, B.C., Jackson, M.R., and Hedrick, S.M. (1994). $\gamma\delta$ T cells can recognize nonclassical MHC in the absence of conventional antigenic peptides. *J. Immunol.* 153, 3051–3058.
- Wilhelm, M., Kunzmann, V., Eckstein, S., Reimer, P., Weissinger, F., Ruediger, T., and Tony, H.P. (2003). Gammadelta T cells for immune therapy of patients with lymphoid malignancies. *Blood* 102, 200–206.
- Xu, C., Gagnon, E., Call, M.E., Schnell, J.R., Schwieters, C.D., Carman, C.V., Chou, J.J., and Wucherpfennig, K.W. (2008). Regulation of T cell receptor activation by dynamic membrane binding of the CD3e cytoplasmic tyrosine-based motif. *Cell* 135, 702–713.

Cell Reports, Volume 7

Supplemental Information

**The CD3 Conformational Change in the $\gamma\delta$ T Cell
Receptor Is Not Triggered by Antigens, but Can
Be Enforced to Enhance Tumor Killing**

Elaine P. Dopfer, Frederike A. Hartl, Hans-Heinrich Oberg, Gabrielle M. Siegers,
Sascha Yousefi, Sylvia Kock, Gina J. Fiala, Beatriz Garcillán, Andrew
Sandstrom, Balbino Alarcón, Jose R. Regueiro, Dieter Kabelitz, Erin J. Adams,
Susana Minguet, Daniela Wesch, Paul Fisch, and Wolfgang W.A. Schamel

The CD3 conformational change in the $\gamma\delta$ T-cell receptor is not triggered by antigens, but can be enforced to enhance tumor killing

Supplemental Figures

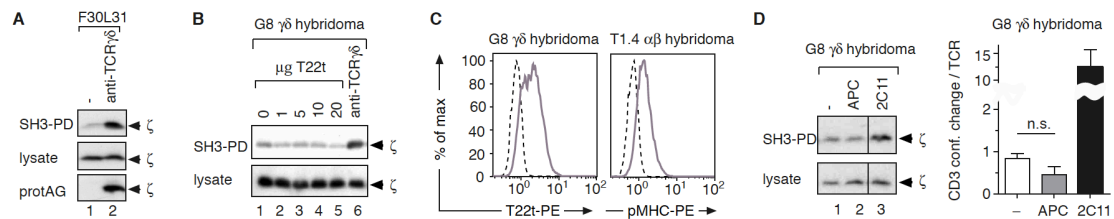


Figure S1, related to Figure 1. CD3 CC induction in murine $\gamma\delta$ TCRs.

(A) The murine $\gamma\delta$ T-cell hybridoma F30L31 was stimulated for 5 min at 37°C with 5 $\mu\text{g/ml}$ of the anti-TCR $\gamma\delta$ mAb GL3. After lysis, one part of the lysates was incubated with SH3-beads and another part with protein A- and protein G-beads. Lysates and bead-purified proteins were analyzed by anti- ζ WB. This experiment shows that the murine $\gamma\delta$ TCR can undergo the CD3 CC upon anti-TCR $\gamma\delta$ mAb stimulation.

(B) G8 $\gamma\delta$ T cells were stimulated with 1, 5, 10 and 20 $\mu\text{g/ml}$ T22t or 5 $\mu\text{g/ml}$ anti-TCR $\gamma\delta$ mAb (GL3) for 5 min, and the SH3-PD assay was performed. This titration of the T22 tetramer suggested that tetramer binding to the G8 $\gamma\delta$ TCR significantly reduced the CD3 CC at different ligand concentrations, as compared to the basal level.

(C) G8 $\gamma\delta$ hybridoma cells were incubated with 5 $\mu\text{g/ml}$ T22 tetramers and T1.4 $\alpha\beta$ hybridoma cells with 5 $\mu\text{g/ml}$ H2-K^d-pepABA tetramers. Both tetramers were prepared from the same stock of PE-labelled streptavidin, thus the PE fluorescence measured by flow cytometry can be compared. Unstained cells served as a negative control. This experiment shows that binding of the G8 $\gamma\delta$ hybridoma cells to T22 tetramers is comparable to that of T1.4 $\alpha\beta$ hybridoma cells binding to pMHC tetramers.

(D) The G8 $\gamma\delta$ hybridoma was kept unstimulated or stimulated for 1 hr at 37°C with LPS-activated splenic B cells from a CD3 ϵ -deficient mouse or with 2C11. The SH3-PD was performed as before. The significance between unstimulated and APC-stimulated cells was determined by the Student's t-test; ns: non significant. This experiment shows that stimulation of the G8 $\gamma\delta$ TCR by its natural ligand T22 did not induce the CD3 CC. We detected a small reduction in the basal CD3 CC suggesting again that T22 had a small impact on the $\gamma\delta$ TCR conformation.

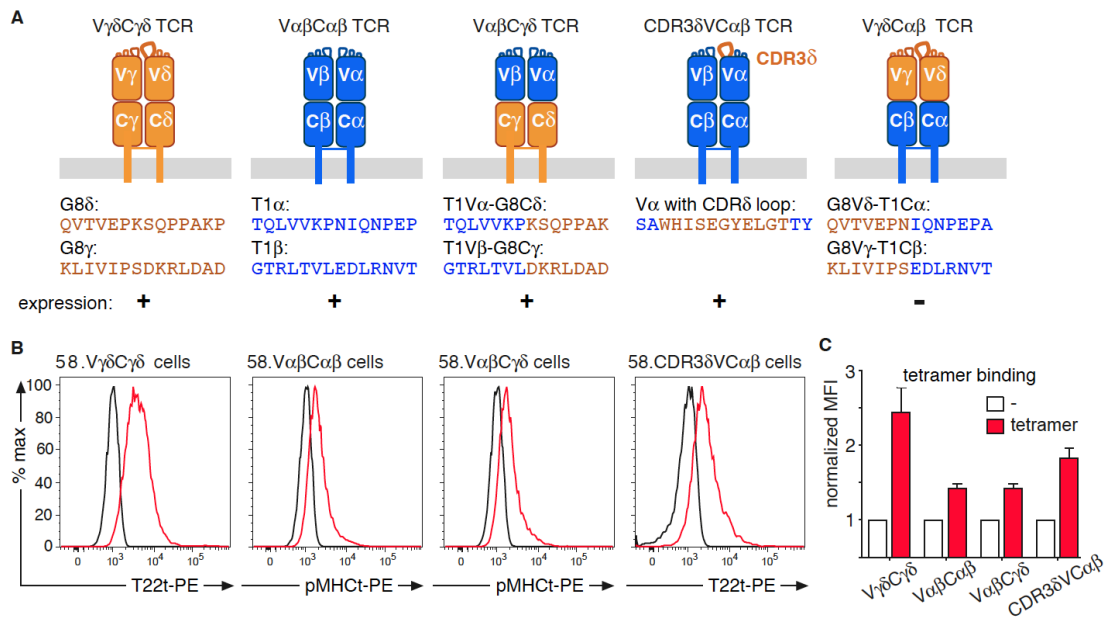


Figure S2, related to Figure 2. Expression of chimeric $\gamma\delta$ - $\alpha\beta$ TCRs.

(A) Schematic of the murine wt and chimeric TCRs used in figure 2. The domains of the G8 $\gamma\delta$ TCR are depicted in beige, including the T22-binding CDR3 δ loop derived from the G8 $\gamma\delta$ TCR; the $\alpha\beta$ TCR domains are in blue. The amino acid sequences are shown below each TCR in the same colour code as in the pictures. The CDR3 δ V C α β TCR was published before (Adams et al., 2008).

58 $\alpha\beta^-$ T cells were lentivirally infected with vectors encoding for the wt or chimeric TCRs. A flow cytometric analysis using the anti-CD3 mAb 2C11 demonstrated that all receptors except the V $\gamma\delta$ C $\alpha\beta$ TCR were expressed on the cell surface. Thus, the 58.V $\gamma\delta$ C $\alpha\beta$ cells were excluded from any further analysis.

(B) The lentivirally infected 58 $\alpha\beta^-$ T cells were stained with 5 μ g/ml PE-labelled T22 tetramers or H2-K^d-pepABA (pMHC) tetramers and analysed by flow cytometry (red lines). Unstained cells served as a negative control (black line). This Experiment shows that the wt and chimeric TCRs bind to their respective tetrameric antigens.

(C) The experiment as in (B) was repeated 13 times. The mean fluorescence intensity (MFI) normalized to the unstained cells \pm standard error of the mean (SEM) is shown. The higher binding capacity of the 58.V $\gamma\delta$ C $\gamma\delta$ and 58.CDR3 δ V C α β cells compared to the 58.V $\alpha\beta$ C $\alpha\beta$ and 58.V $\alpha\beta$ C $\gamma\delta$ cells, could be due to the higher affinity of the T22-G8 $\gamma\delta$ TCR interaction.

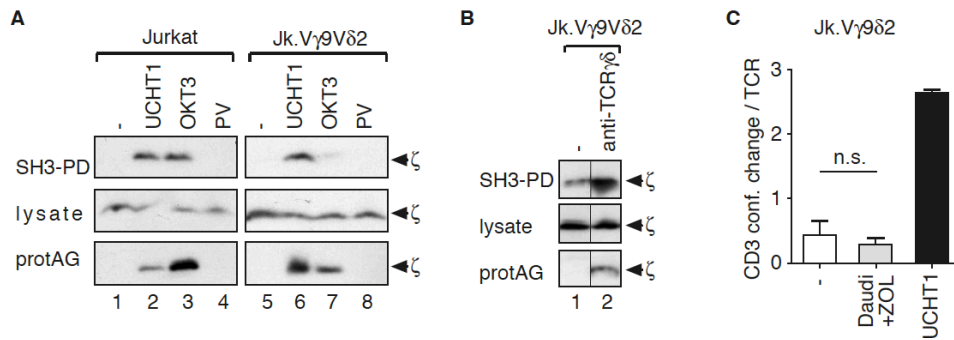


Figure S3, related to Figure 3. Induction of the CD3 CC at the human $\gamma\delta$ TCR.

(A) Jurkat ($\alpha\beta$ TCR-expressing) and Jk.V γ 9V δ 2 ($\gamma\delta$ TCR-expressing) cells were left untreated (-) or stimulated for 5 min at 37°C with 5 μ g/ml of the anti-CD3 mAbs UCHT1 and OKT3 or pervanadate (PV). After lysis the SH3-PD assay was performed (n=3).

(B) Jk.V γ 9V δ 2 cells were left untreated or stimulated for 5 min at 37°C with 5 μ g/ml of anti-TCR $\gamma\delta$ mAbs. After lysis the SH3-PD was performed (n=2).

(C) Jk.V γ 9V δ 2 cells were stimulated in triplicate as in main figure 3E. The ratio of SH3-bound TCR to total TCR (ζ) was calculated using the Odyssey infrared imager. The mean \pm standard deviation (SD) is shown. Significance between unstimulated and cells stimulated with Daudi+ZOL was determined by the Student's t-test; n.s. = not significant.

These experiments demonstrate that UCHT1 and anti-TCR $\gamma\delta$ mAbs, but neither OKT3 nor ZOL-pulsed Daudi cells, trigger the CD3 CC in a $\gamma\delta$ TCR independent of the cellular environment.

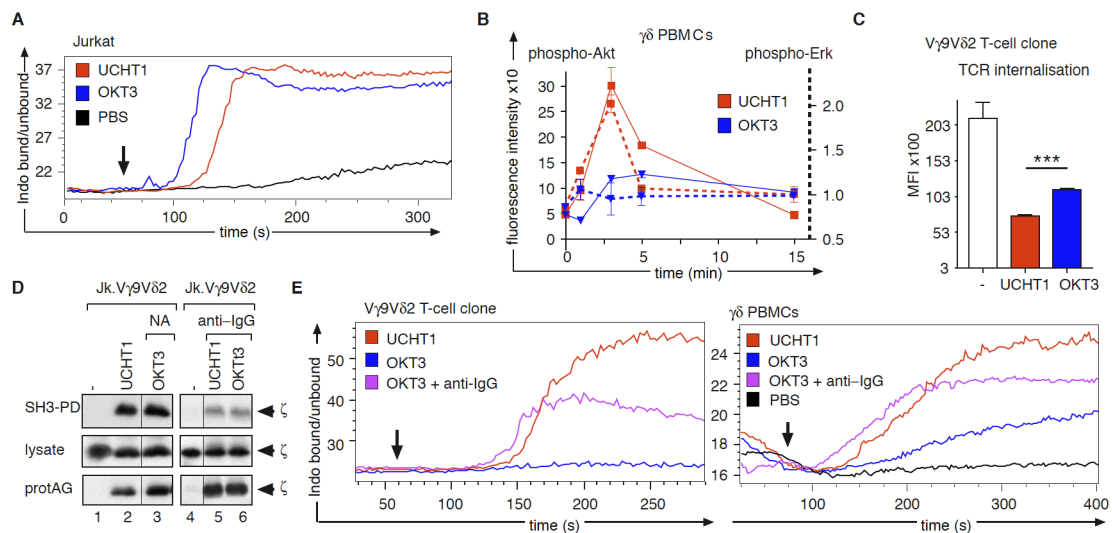


Figure S4, related to Figure 4. Induction of the CD3 CC in $\gamma\delta$ TCRs promotes proximal signalling.

(A) Jurkat cells were loaded with Indo-1 and stimulated with 5 μ g/ml of the anti-CD3 mAbs UCHT1 and OKT3. The Indo-1 ratio was integrated over 6 min and measured by flow cytometry, showing that both mAbs induce Ca^{2+} -influx in $\alpha\beta$ T cells. This is in line with the capacity of both mAbs to induce the CD3 CC in the $\alpha\beta$ TCR.

(B) Human freshly isolated, untouched purified $\gamma\delta$ T cells ($\gamma\delta$ PBMCs) were stimulated with 5 μ g/ml UCHT1 and OKT3 for 1, 3, 5 and 15 min. Phospho-Akt (solid line, y-axis on left) and phospho-Erk (dashed line, y-axis on right) were measured by a multiplexed-bead assay performed on cell lysates.

(C) The V γ 9V δ 2 T-cell clone was stimulated in triplicates for 4 hr with 5 μ g/ml soluble UCHT1 or OKT3. Subsequently, cells were stained with anti-TCR $\gamma\delta$ (5A6E9) mAb for flow cytometry. Significances between UCHT1- and OKT3-stimulated cells were determined by the Student's t-test; ***: $p < 0.001$. This experiment shows that UCHT1 induces stronger $\gamma\delta$ TCR downmodulation than OKT3.

(D) Jk.V γ 9V δ 2 cells were left untreated or deglycosylated with N-acetyl neuraminidase (NA) for 1 hr at 37°C (left). Subsequently, cells were stimulated with 5 μ g/ml UCHT1 or OKT3 for 5 min. Jk.V γ 9V δ 2 T cells were stimulated with 5 μ g/ml UCHT1 or OKT3 in the presence of an anti-IgG antibody (2.5 μ g/ml, right). After cell lysis the SH3-PD was performed. Thus, a $\gamma\delta$ TCR expressed in an $\alpha\beta$ T cell undergoes the CD3 CC upon OKT3 stimulation when deglycosylated. In addition, multimerization of OKT3 promotes CD3 CC induction.

(E) The V γ 9V δ 2 $\gamma\delta$ T clone (left panel) or human freshly isolated, untouched purified $\gamma\delta$ T cells ($\gamma\delta$ PBMCs, right panel) were loaded with Indo-1 and stimulated with 5 μ g/ml UCHT1 or OKT3 with or without 2.5 μ g/ml anti-IgG and Ca^{2+} influx was measured as in (A). This result demonstrates that supplementing OKT3 stimulation with the CD3 CC by multimerizing with an anti-IgG antibody leads to Ca^{2+} -influx.

The experiments shown in all panels were done at least three times ($n=3$).

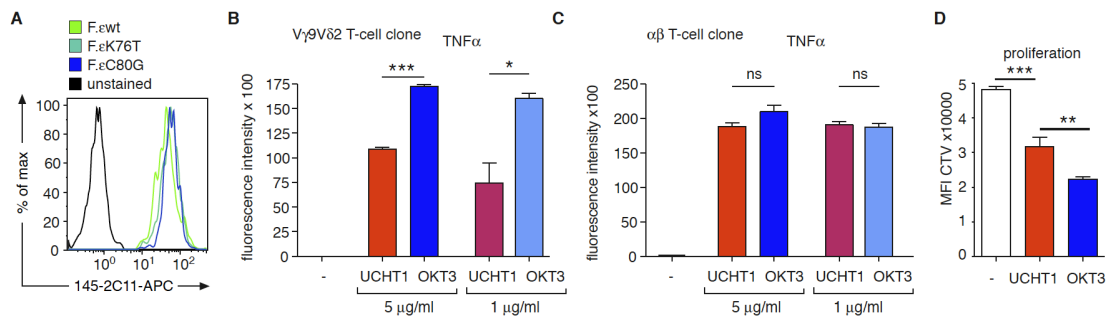


Figure S5, related to Figure 6. TNF α production by a $\gamma\delta$ and $\alpha\beta$ clone stimulated with UCHT1 and OKT3.

(A) The murine $\gamma\delta$ T-cell line F30L31 exogenously expressing CD3 ϵ wt, CD3 ϵ K76T or CD3 ϵ C80G was stained with an APC-labelled anti-CD3 mAb 145-2C11 and analysed by flow cytometry. The histogram shows that all three lines express similar levels of $\gamma\delta$ TCR.

(B) The human V γ 9V δ 2 $\gamma\delta$ T-cell clone was left untreated (-) or stimulated with UCHT1 or OKT3 using 5 μ g/ml or 1 μ g/ml for 20 hours as indicated. The cellular supernatants were used to measure TNF α by a multiplexed bead assay.

(C) The human $\alpha\beta$ T-cell clone was stimulated as in (A). TNF α in the cellular supernatant was measured as in (A). Together, these data show that the difference in the activity of UCHT1 and OKT3 in $\gamma\delta$ T cells (Figure 5D) is not detected in $\alpha\beta$ T cells. Significances between UCHT1- and OKT3-stimulated cells in (B) and (C) were determined by the Student's t-test; ***: $p < 0.001$; *: $p < 0.05$; ns: non significant.

(D) A primary $\gamma\delta$ T-cell culture was labelled with 1 μ M Cell Trace Violet and left unstimulated or stimulated with 5 μ g/ml soluble UCHT1 or OKT3 as indicated. After 4 days proliferation was determined by flow cytometry. Quantification of the mean fluorescence intensity (MFI) of triplicates is given ($n=3$).

Mean \pm SD of triplicates is shown. Significances between unstimulated and UCHT-stimulated cells as well as between UCHT1- and OKT3-stimulated cells were determined by the Student's t-test; ns: not significant; **: $p < 0.01$; ***: $p < 0.001$.

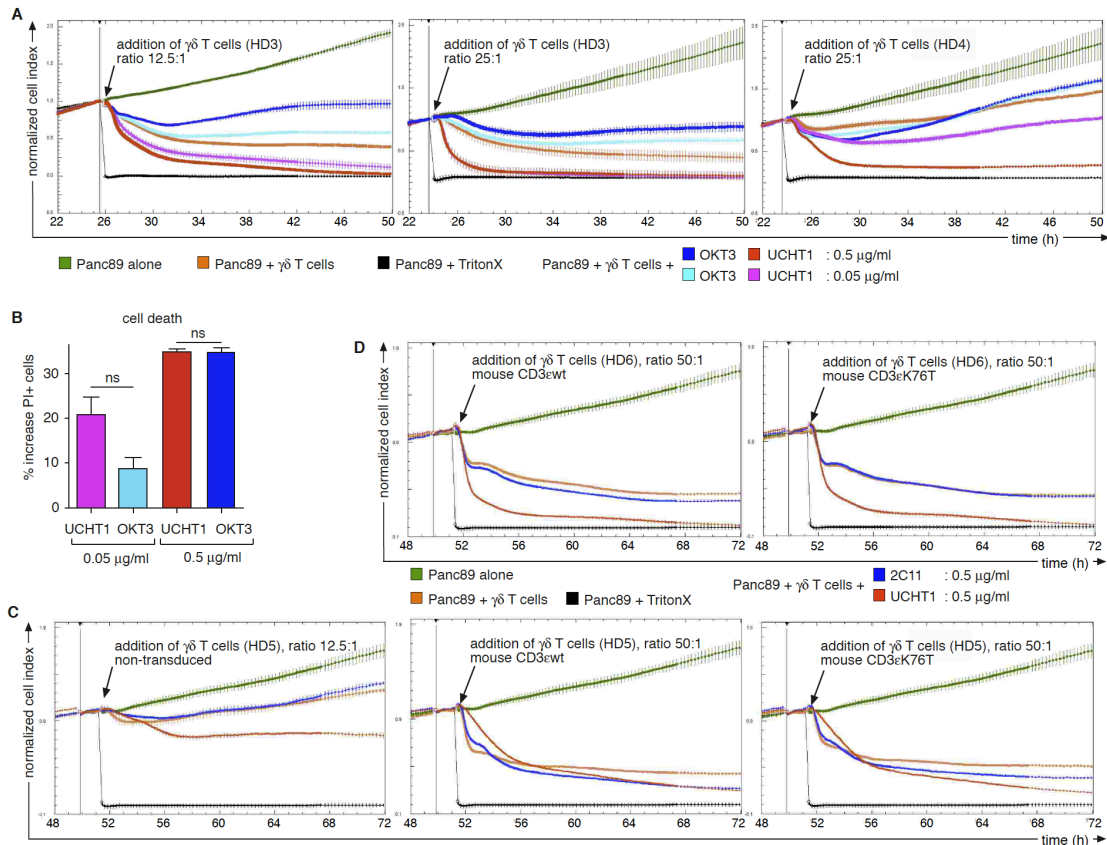


Figure S6, related to Figure 7. Induction of the CD3 CC increases $\gamma\delta$ T cell-mediated tumor cell lysis. **(A)** The growth of Panc89 tumor cells was measured as shown in figure 7. After 24 hr human short-term activated V γ 9V δ 2 T-cell lines from healthy donor (HD) 3 or HD4 (as indicated) in medium (orange) or together with the indicated concentrations of the mAbs UCHT1 or OKT3 were added to the assay. The effector target ratio was 12.5:1 (left panel) or 25:1 (middle and right panels). Growth of the tumor cells alone (green) or lysis by detergent (black) are shown as controls. These experiments corroborate the finding of figure 7 that UCHT1, in contrast to OKT3, enhances $\gamma\delta$ T cell-mediated tumor cell lysis. **(B)** Human V γ 9V δ 2 T-cell lines of the three donors in figure 7 were cultured with medium alone or in the presence of UCHT1 and OKT3 mAbs as indicated. Propidiumiodide positive (PI⁺) cells were determined after 24 hr by flow cytometry. Mean \pm SD of three experiments is shown. Significances between UCHT1- and OKT3-stimulated cells were determined by the Student's t-test; ns: non significant. The experiment demonstrates that both mAbs induce a similar level of activation-induced apoptosis. **(C)** A human short-term activated V γ 9V δ 2 T-cell line was either left untreated (left panel), or lentivirally transduced with CD3 ϵ wt (middle panel) or with CD3 ϵ K76T (right panel). After 3 days, the viruses were removed and after another 2 days the growth of the Panc89 cells in the presence or absence of the $\gamma\delta$ T cells was measured as in (A) with or without addition of the anti-mouse CD3 ϵ mAb 2C11. As a control, stimulation with 2C11 did not have any effect the parental V γ 9V δ 2 cells that do not express mouse CD3 ϵ . In cells expressing CD3 ϵ wt the anti-tumoral activity was enhanced compared to cells expressing CD3 ϵ K76T. **(D)** The experiment was done as in (C) using a V γ 9V δ 2 T-cell line from a different donor. In contrast to (C) where the expression levels of CD3 ϵ wt and CD3 ϵ K76T were the same (see main text), CD3 ϵ wt was expressed slightly better than CD3 ϵ K76T (MFI of the 2C11 stain of 65 and 48, respectively). Stimulation of CD3 ϵ wt-expressing cells with 2C11 could enhance the cytotoxic activity of the cells, whereas stimulation of CD3 ϵ K76T-expressing cells could not. The experiments in (C) and (D) suggest that expression of murine CD3 ϵ and stimulation with 2C11 can enhance the cytotoxicity of these human $\gamma\delta$ T cells, and that a reduced capacity to undergo the CD3 CC reduces the anti-tumoral activity. Thus, the CD3 CC is required for efficient tumor killing.

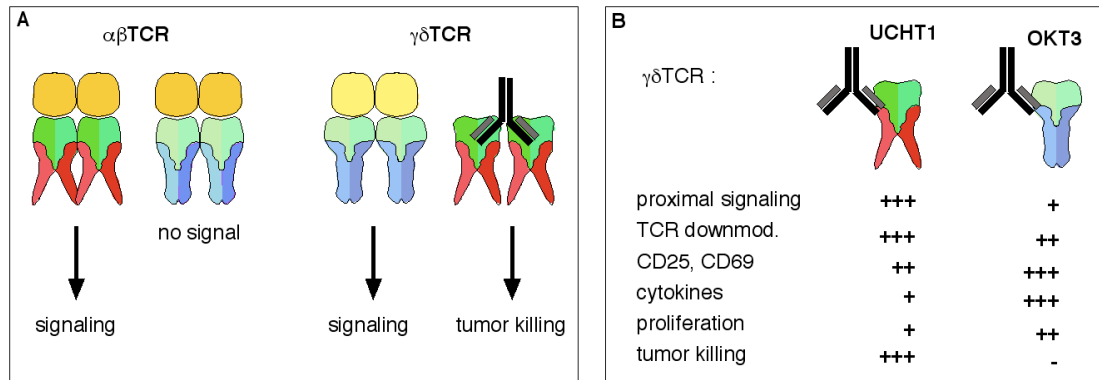


Figure S7, related to Figures 4, 6 and 7. Influence of the CD3 CC on $\gamma\delta$ TCR signaling.

(A) Activation of the $\alpha\beta$ TCR requires CD3 CC induction (red CD3 tails) by antibody/antigen (orange). Without induction of the CD3 CC by artificial ligands or in a mutated TCR the $\alpha\beta$ TCR is not activated (blue CD3 tails). In contrast, several activation events mediated by the three $\gamma\delta$ TCRs studied here did not require the CD3 CC and the $\gamma\delta$ T-cell antigens tested (yellow) did not induce this change. However, artificial induction of the CD3 CC did enhance tumor killing by $\gamma\delta$ T cells. **(B)** The mAb UCHT1 triggers the CD3 CC in the human V γ 9V δ 2 TCR, whereas OKT3 does not. Stimulation of the $\gamma\delta$ TCR with UCHT1 results in strong proximal signaling and TCR downmodulation, upregulation of the activation markers CD25 and CD69, weak cytokine secretion and massive tumor killing. In contrast, stimulation with OKT3 hardly induces proximal signaling and TCR downmodulation, upregulates CD25, CD69 and cytokines, promotes proliferation but inhibits tumor killing by the V γ 9V δ 2 T cells. These findings were confirmed using mutant CD3 ϵ chains that cannot undergo the CD3 CC.

Supplemental Experimental Procedures

Cells and mice. The human V γ 9V δ 2 T-cell clone ($\gamma\delta$ PF55) was generated and maintained as described (Fisch et al., 1990; Fisch et al., 1997). JK.V γ 9V δ 2 T cells were generated from TCR $\alpha\beta^{-/-}$ Jurkat T cells transfected with TCR V γ 9 and TCR V δ 2 (Alibaud et al., 2001). The murine $\gamma\delta$ T-cell hybridomas G8 and F30L31 were obtained from Y.H. Chien, Stanford, USA, and K. Eichmann, Freiburg, Germany, respectively, and the murine $\alpha\beta$ T-cell hybridoma 2B4 from J. Ashwell, Bethesda. The pancreatic ductal adenocarcinoma cell line Panc89 was provided by H. Kalthoff, Section of Molecular Oncology, UKSK, Campus Kiel, Germany. All cells were maintained in RPMI 1640 medium supplemented with 10% fetal bovine serum. TCR $\beta^{-/-}$ V γ 1.1V δ 6 transgenic mice have been previously described (Siegers et al., 2007). The CD3 ϵ knock out mouse was described before (DeJarnette et al., 1998). Mice were killed between 6 and 12 weeks of age and lymphocytes were isolated from the indicated tissues according to standard protocols. Human $\gamma\delta$ peripheral blood mononuclear cells ($\gamma\delta$ PBMCs) were isolated from a healthy donor using a Ficoll-Hypaque gradient followed by negative isolation using the human TCR γ/δ + untouched T-Cell Isolation Kit human (Miltenyi Biotech) to enrich the $\gamma\delta$ T cells.

Mouse experiments were approved by the relevant institutional review boards (code number: T-02/31). Informed consent was obtained from all human blood donors, and the research was approved by the relevant institutional review boards (code number: D 405/10).

Short-time cultured human $\gamma\delta$ T-cell lines were used in the tumor cell killing assays. To this end, PBMCs from healthy donors were cultured in RPMI 1640 supplemented with 10 % fetal calf serum, and then stimulated with 5 μ mol/l of aminobisphosphonate zoledronic acid (Novartis) and 50 U/ml rIL-2 (Novartis). Additionally, rIL-2 was added every two days over a culture period of 20 days. The purity of expanded $\gamma\delta$ T cells was analyzed by flow cytometry and was > 97% V γ 9V δ 2 T cells.

Antibodies, antigens and reagents. The rabbit anti- ζ antiserum 448 was described (San Jose et al., 1998). UCHT1 (anti-hCD3 ϵ) was provided by P. Beverly, London, U.K. The following reagents were purchased: OKT3 hybridome (anti-hCD3 ϵ , American Type Culture Collection), GL3-PE (anti-mTCR $\gamma\delta$, eBiosciences), 5A6.E9-PE (anti-hTCR $\gamma\delta$, Invitrogen), 145-2C11 (anti-mCD3 ϵ , eBioscience), anti-hCD69-APC (Invitrogen), anti-hCD25-PE, goat anti-rabbit IgG-HRPO (both, Pierce), and anti- κ and anti-IgG (Southern Biotech). Zoledronate was supplied as hydrated disodium salt by Novartis Pharma. BrHPP was kindly provided by Innate Pharma. T22 monomers were expressed and purified as previously described (Adams et al., 2008). H2-K^d-pepABA (pMHC) monomers were obtained from TCMetrix. PE-coupled streptavidin (Life Technologies) was used to generate the T22 and pMHC tetramers.

Cloning and expression of the chimeric TCRs. The CDR3 δ VC $\alpha\beta$ TCR has been published (Adams et al., 2008). Here we inserted before the start codon of CDR3 δ 172 α or 172 β with a fusion-PCR a XhoI restriction site and a mouse TCR δ leader peptide sequence. A stop codon was inserted at the original place followed by a XbaI restriction site. The resulting PCR products were cloned into pLVX-IRES-ZsGreen1 (Clontech Lab). TCR $\alpha\beta$ ⁻ cells were transduced with virus containing CDR3 δ 172 α or 172 β plasmids and plated to obtain single clones. Transduced cells were tested for TCR expression by anti-CD3 (2C11) flow cytometry. The CMV promoter of the lentiviral vector pLVX-IRES-ZsGreen1 (Clontech Lab) was exchanged by the SFFV promoter from the pHR SIN CSGW plasmid. Furthermore, the ZsGreen1 cDNA was exchanged by either the cDNA of the puromycin N-acetyl-transferase (from pIRESpuro3, Clontech Lab) or of the hygromycin B phosphotransferase (pLHCX, Clontech Lab). Thus, three lentiviral backbones were obtained: pLVX-S IZ, pLVX-S IP and pLVX-S IH (pLVX with the SFFV promoter and either IRES-ZsGreen1, IRES-puromycin resistance or IRES-hygromycin B resistance, respectively).

For the V $\alpha\beta$ C $\alpha\beta$ TCR, the sequences encoding the TCR α and TCR β chains of the T1 $\alpha\beta$ TCR were amplified from cDNA of the T1.4 hybridoma cells. The TCR α sequence was cloned into pLVX-S IP and the TCR β sequence into pLVX-S IH. The cDNAs of the V $\gamma\delta$ C $\gamma\delta$ TCR (G8 TCR γ and G8 TCR δ sequences) were cloned into the same vectors. The chimeric V $\alpha\beta$ C $\gamma\delta$ and V $\gamma\delta$ C $\alpha\beta$ TCRs were generated by joining the T1 TCR α and G8 TCR δ sequences, as well as the T1 TCR β and G8 TCR γ sequences at the V-C borders as defined by the respective exons (see also Figure S2A). For each chimeric TCR, one sequence was cloned into pLVX-S IP and the other one into pLVX-S IH. All constructs were verified by sequencing.

58 $\alpha\beta$ ⁻ cells were transduced with lentivirus supernatants encoding for both chains and co-transduced cells were selected with puromycin (PAA) and hygromycin B (Invitrogen). Transduced cells were tested for TCR expression by anti-CD3 (2C11) flow cytometry.

Cloning and expression of the mutant CD3 ϵ molecules. Murine CD3 ϵ wild-type as well as the CD3 ϵ K76T mutant sequences were amplified from pHR SIN CSGW plasmids and cloned into pLVX-S IZ. The CD3 ϵ C80G mutant sequence was derived from the wt CD3 ϵ sequence by site-directed mutagenesis. All constructs were verified by sequencing. F30L31 and human $\gamma\delta$ T cells were transduced with lentivirus encoding for the wt or mutant CD3 ϵ chains.

Proliferation assay. $\gamma\delta$ T-cell cultures derived from healthy donor PBMC were generated as described (Siegers et al., 2012). On day 9, $\gamma\delta$ T cells were labeled with 1 μ M Cell Trace Violet (CTV, Invitrogen, Burlington, Canada) and resuspended at 10⁶ cells/ml in complete medium: RPMI 1640 with 10% fetal bovine serum, 1x MEM NEAA, 10 mM HEPES, 1 mM

sodium pyruvate (all Gibco/Life Technol) containing 10 ng/ml recombinant IL-2 (rIL-2, Proleukin, Novartis Pharmaceuticals, Canada) and 10 ng/ml IL-4 (Life Technol). Cells were untreated, or stimulated with 5 µg/ml anti-human CD3 mAb UCHT1 or OKT3 (Biolegend) and plated at 200 µl/well in a 96-well round bottom plate (BD Biosciences).

Apoptosis assay. 250,000 human freshly isolated, purified $\gamma\delta$ T cells were cultured with medium alone or with the indicated stimuli for 24 hr. Propidium iodide positive (PI⁺) cells were determined in all cultures after 24 hr by flow cytometry using a FACSCalibur. Results are presented as enhancement of OKT3- or UCHT-1 mAb mediated cell death beyond the medium control.

Supplemental References

Adams, E.J., Strop, P., Shin, S., Chien, Y.H., and Garcia, K.C. (2008). An autonomous CDR3 δ is sufficient for recognition of the nonclassical MHC class I molecules T10 and T22 by $\gamma\delta$ T cells. *Nat Immunol* 9, 777-784.

Alibaud, L., Arnaud, J., Llobera, R., and Rubin, B. (2001). On the role of CD3 δ chains in TCR $\gamma\delta$ /CD3 complexes during assembly and membrane expression. *Scand J Immunol* 54, 155-162.

DeJarnette, J.B., Sommers, C.L., Huang, K., Woodside, K.J., Emmons, R., Katz, K., Shores, E.W., and Love, P.E. (1998). Specific requirement for CD3epsilon in T cell development. *Proc Natl Acad Sci U S A* 95, 14909-14914.

Fisch, P., Malkovsky, M., Kovats, S., Sturm, E., Braakman, E., Klein, B.S., Voss, S.D., Morrissey, L.W., DeMars, R., Welch, W.J., *et al.* (1990). Recognition by human V γ 9/V δ 2 T cells of a GroEL homolog on Daudi Burkitt's lymphoma cells. *Science* 250, 1269-1273.

Fisch, P., Meuer, E., Pende, D., Rothenfusser, S., Viale, O., Kock, S., Ferrone, S., Fradelizi, D., Klein, G., Moretta, L., *et al.* (1997). Control of B cell lymphoma recognition via natural killer inhibitory receptors implies a role for human V γ 9/V δ 2 T cells in tumor immunity. *Eur J Immunol* 27, 3368-3379.

San Jose, E., Sahuquillo, A.G., Bragado, R., and Alarcon, B. (1998). Assembly of the TCR/CD3 complex: CD3 epsilon/delta and CD3 epsilon/gamma dimers associate indistinctly with both TCR alpha and TCR beta chains. Evidence for a double TCR heterodimer model. *Eur J Immunol* 28, 12-21.

Siegers, G.M., Ribot, E.J., Keating, A., and Foster, P.J. (2012). Extensive expansion of primary human gamma delta T cells generates cytotoxic effector memory cells that can be labeled with Feraheme for cellular MRI. *Cancer Immunol Immunother* 62, 571-583.

Siegers, G.M., Swamy, M., Fernandez-Malave, E., Minguet, S., Rathmann, S., Guardo, A.C., Perez-Flores, V., Regueiro, J.R., Alarcon, B., Fisch, P., *et al.* (2007). Different composition of the human and the mouse $\gamma\delta$ T cell receptor explains different phenotypes of CD3 γ and CD3 δ immunodeficiencies. *J Exp Med* 204, 2537-2544.